2015

Validation of Ndesign in Iowa

Marie Grace Joson Mercado
Iowa State University

Validation of N_{design} in Iowa

by

Marie Grace Joson Mercado

A thesis submitted to the graduate faculty

in partial fulfillment of the requirements for the degree of

MASTER OF SCIENCE

Major: Civil Engineering (Civil Engineering Materials)

Program of Study Committee:
R. Christopher Williams, Major Professor
Ashley F. Buss
Vernon R. Schaefer
Derrick K. Rollins

Iowa State University

Ames, Iowa

2015

TABLE OF CONTENTS

LIST OF FIGURES iv

LIST OF TABLES v

ACKNOWLEDGEMENTS vi

ABSTRACT vii

CHAPTER 1: INTRODUCTION 1

Background 1

Problem Statement 2

Objectives 3

Methods and Approach 3

Significance of Work 4

Organization 4

CHAPTER 2: LITERATURE REVIEW 5

History of Asphalt Mix Design 5

Comparison of the mix design methods 8

Superpave N_{design} 10

The significance of N_{design} 10

Disadvantages/Issues 11

Validation of N_{design} 12

NCHRP Report 573 12

Gyratory Locking Point (LP) 14

$N_{initial}$ and $N_{maximum}$ 15

NCHRP Recommendations 16

Reduction of N_{design} in other States 17

Effects on Pavement Performance 19

Rutting 20

Fatigue Cracking 21

Thermal Cracking 23

CHAPTER 3: EXPERIMENTAL PLAN AND TESTING METHODS 24

Introduction and Overview 24

Project Selection 26

Evaluation of Existing Pavement Conditions 29

Flexible Pavement Distresses 29

Selection and determination of pavement condition using PMIS 31
Determination of Field Densities 33
Evaluation of the Gyratory Slope and Post-Construction Compaction effort (PCCE) 36
CHAPTER 4: RESULTS AND ANALYSES 38
Pavement Performance Evaluation using PMIS and LTPP 38
1 Million ESALS 39
3 Million ESALs 42
10 Million ESALs 44
Theoretical maximum specific gravity QC/QA versus AASHTO T 209 47
Change in Air Voids post-construction 48
Air Voids at construction and four years post-construction 52
Gyratory compaction slope and Post Construction Compaction Effort (PCCE) 53
CHAPTER 5: CONCLUSIONS AND RECOMMENDATIONS 59
REFERENCES 62
APPENDIX A: QC/QA FIELD VOIDS DATA 64
APPENDIX B: QC/QA LABORATORY DATA 66
APPENDIX C: RAW DATA FOR AIR VOID ANALYSES 69

LIST OF FIGURES

Figure 1: Typical Superpave mixes 6
Figure 2: HMA compaction device. Left: California kneading compactor. Middle: Marshall hammer. Right: Superpave Gyratory Compactor (FHWA) 9
Figure 3: Pine Instrumental Company, AFG2AS/AFG2CS Superpave Gyratory Compactor. [1] 9
Figure 4: Stress distribution of flexible pavement [2] 11
Figure 5: Location of NCHRP Project 9-9 field studies [4] 13
Figure 6: Illinois 3-2-2 locking point [4] 15
Figure 7: Concept of N_{design} 16
Figure 8: FMLC versus FMFC Air Voids after 3 Years [3] 19
Figure 9: Severe rutting in flexible pavement [19] 20
Figure 10: Fatigue cracking (left). Pothole caused by fatigue cracking (right) [20] 22
Figure 11: Block cracking, type of thermal cracking [21] 23
Figure 12: Flow chart of experimental plan for the study 25
Figure 13: Identification of field sections in Iowa, specific project locations in Iowa 27
Figure 14: Cumulative distribution of surface mixes 29
Figure 15: Actual field core samples 33
Figure 16: Corelock method 34
Figure 17: Water bath used for conventional method 35
Figure 18: Metal bucket method (left) and flask method (right) 36
Figure 19: Conceptual representation of theoretical post-construction compaction effort (PCCE) 37
Figure 20: At 1M ESALs. (a) Alligator or Fatigue cracking, (b) Transverse cracking, (c) Longitudinal cracking, (d) Rutting 41
Figure 21: At 3M ESALs. (a) Alligator or Fatigue cracking, (b) transverse cracking, (c) longitudinal cracking, (d) rutting 43
Figure 22: At 10M ESALs. (a) Alligator or Fatigue cracking, (b) transverse cracking, (c) longitudinal cracking, (d) rutting 45
Figure 23: IRI indication at each ESAL levels 46
Figure 24: G_{mm} estimated or QC/QA versus actual G_{mm} or G_{mm} tested with AASHTO T209 47
Figure 25: Calculated air voids with estimated G_{mm} from QC/QA data and air voids with G_{mm} measured from the field core tested in accordance to AASHTO T209 48
Figure 26: Change in percent air voids per ESAL level, (a) 100-300K, (b) 1M, (c) 3M, and (d) 10M 50
Figure 27: Change in percent air voids against ESALs (left). Distribution of the percent change in air voids with varying ESAL levels (right). 51
Figure 28: Average AV at construction and four years post-construction 51
Figure 29: Percent air voids at construction versus air voids four years post-construction 53
Figure 30: Post-construction compaction effort (PCCE) per ESAL level 55
Figure 31: Average Theory $N_{@4yrs}$, $N_{@const.}$, and PCCE for each ESAL level 56
Figure 32: Distribution of % G_{mm} at construction with an expected shifted distribution for air voids at four years post-construction 58

LIST OF TABLES

Table 1: NCHRP Compaction Parameters [8] 8
Table 2: NCHRP Recommended Ndesign Levels for SGC DIA of 1.16° ± 2 [4]. 17
Table 3: Project location for the study 28
Table 4: Level of severity corresponding type of distress [22] 30
Table 5: Project selected to evaluate pavement condition 32
Table 6: Compaction slope from mix data 55
Table 7: QC/QA field voids data for selected projects 64
Table 8: Cont. of QC/QA field voids data for selected projects 65
Table 9: QC/QA laboratory voids data for selected projects 66
Table 10: Cont. of QC/QA laboratory voids data for selected projects 67
Table 11: Cont. of QC/QA laboratory voids for selected projects 7-12 68
Table 12: Data for air void analyses 69
Table 13: Cont. of data for air void analyses 70

ACKNOWLEDGEMENTS

I would first like to thank God for the continuous blessings and for providing me with great opportunities. I would like thank and express my sincere gratitude to my major professor Dr. R. Christopher Williams for his continuous support and guidance. He challenged, encouraged and pushed me to produce the best quality work. I am also grateful for Dr. Ashley Buss, my mentor in senior design and graduate committee member, for her patience, support and her time. Her guidance and support helped me tremendously in both my undergraduate and graduate studies. I would like to also thank my Dr. Vernon Schaefer R. and Dr. Derrick K. Rollins for being part of my graduate committee. Thank you Dr. Schaefer for the advice, support, and humorous conversations. And also, Dr. Rollins Derrick K., for his continuous support, guidance and sincere motivation.

More importantly, I would like to thank my family and friends. I would like to thank my father, Maximino C. Mercado and mother, Josie Socorro R. Mercado for their continuous support; financially, emotionally, and mentally. I hope to make you both proud. I am grateful for such supportive parents and siblings who believed in me. And, to Tiffany A. Camarillo, thank you for always being there for me. You've supported me throughout my entire college journey and I would like to sincerely thank you for pushing me to be the best person you know I am capable to be. I am grateful and I am truly blessed to have someone like you in my life, I promise to make you proud.

Special thanks to my graduate colleges, Congling Chen, Zahra Sotoodeh Nia, Parnian Ghasemi, Ka Lai Ng, Paul Ledtje, Jianhua Yu, Joseph Podolsky, Andy Cascione, Joana Peralta and Sirui Guo. Lastly, special thanks to Iowa Department of Transportation (IDOT).

ABSTRACT

The design number of gyrations, or N_{design} introduced by Strategic Highway Research Program (SHRP) used in the Superpave mix Design method has been commonly used in flexible pavement design throughout the United States. The N_{design}, also known as the compaction effort used to simulate field compaction during construction has been reported to produce air voids that are unable to reach ultimate pavement density after some period of time. Other states had conducted studies validating the N_{design} for their specific region. This study will focus on the validation of N_{design} in the State of Iowa. Pavement sections constructed in 2011 were randomly selected to determine if 4% target air voids was being achieved four years post-construction.

The objective of the study is to determine if the current mix design gyratory levels are creating mixes that will reach target densification under traffic. The quality control and quality assurance (QC/QA) information at construction was matched with four year post-construction densities from field cores to determine if traffic loading is adequately compacting the surface mix.

The compaction effort is critical in design. Over-compaction during design may lead to under-compaction in the field as well as reduce asphalt content and affect overall durability. Findings of the study suggest majority of mixes were not achieving 4% air voids four years post-construction and mixes with lower design gyrations compact more readily post-construction even though traffic levels are lower. Majority of the projects in the highest traffic volume were unable to reach ultimate pavement density with the current design gyrations.

CHAPTER 1: INTRODUCTION

Background

The use of asphalt pavements has gradually increased since the late 19th century and covers about 94 percent of paved roads [5]. The mix design of asphalt pavements has undergone continual evolution since initial development, relying heavily on empirical knowledge. Past challenges with pavement distresses in asphalt concrete had shaped design considerations in mix design and analysis. In the U.S., the Superpave mix design is used in majority of the states. One of the most important factors in design is the compaction effort of the asphalt mixture. The compaction effort in the laboratory is known as the number of gyrations and is denoted as $N_{initial}$, N_{design}, and N_{max} in the Superpave mix design. The design number of gyrations or N_{design} is one of the most significant design considerations/parameters in the laboratory and is selected based on the corresponding equivalent single axle load (ESAL) levels for the proposed pavement structure. The initial Superpave values were selected based on studies that matched in-place densities to a number of gyrations conducted by the Strategic Highway Research Program (SHRP) [4].

Over time, many agencies/researchers had performed additional studies to validate gyratory design levels [3]. Previous studies concluded the N_{design} in the Superpave mix design method is considerably higher than necessary and as a result, the compaction effort conducted in the laboratory may not be reasonably attained in the field due to differences in the compaction equipment, compaction procedure, and finally the difficultly to compact in the field. During construction, the pavement is compacted in multiple lifts using rollers. Post-construction compaction is expected to occur overtime from traffic loading to achieve an ultimate pavement

density of four percent air voids over the next two to three years. However, studies have shown that if N_{design} is too high, then ultimate pavement density cannot be achieved within that time frame. The primary reason is the difficulty to compact in the field, which consequently results in under compaction that can cause durability issues in the pavement. In addition, the aging of the asphalt mixture is considerably affected by the initial air voids and temperature during production [5]. Validation of the existing N_{design} table in Superpave mix design will allow agencies to tailor the laboratory mix design process so four percent air voids can be achieved from ultimate density.

As the evolution to modern technology continues to grow rapidly, the industry will need to continuously improve and modify standards to accommodate the changes in traffic volumes, environment, and the automobile and trucks industry. Validation of the existing N_{design} table in the Superpave mix design will allow agencies/researchers to better evaluate the field and laboratory pavement responses more accurately. Ensuring adequate pavement density will reduce pavement distresses and improve overall durability in the pavement.

Problem Statement

The design number of gyrations or N_{design} has been used in the laboratory to compact specimens to a design ESAL level. The existing N_{design} table in the Superpave mix design method has been reported to result in under compaction and lower asphalt content in the field.

Objectives

The objective of the research is to validate current N_{design} levels for one-hundred thousand (100K) to ten million (10M) ESAL surface mix designs. Projects in Iowa from 2011 were randomly selected at each ESAL level to evaluate whether the ultimate in-place density has been achieved. Collection of field cores provided measurements of in-place densities and at four-year post-construction. The second objective is to assess the compactability of mixes under the current mix design procedures by using the gyratory slope from quality control and quality assurance (QC/QA) data. In addition, the post-construction compaction effort (PCCE) will be evaluated. The third objective is to provide N_{design} recommendations for the laboratory used in Superpave mix design to the Iowa Department of Transportation (DOT) based on the findings of this study.

Methods and Approach

The overall study focuses primarily on the laboratory compaction effort or $N_{design.}$ Testing was done in accordance to Superpave mix design methods and procedures. The field cores used for the study were provided by the Iowa Department of Transportation (DOT). In addition to the Superpave mix design methods, laboratory testing was also conducted using ASTM and/or AASHTO standards. The selected projects for the study were randomly chosen throughout the State of Iowa, and varied in traffic volume. Pavement condition surveys were also evaluated based on available data using the Pavement Management Information System (PMIS) surveys and the Long Term Pavement Performance Program (LTPP) manual. Determination of field air voids will be compared to QC/QA data, pre and post-construction will be analyzed accordingly.

In addition, the gyratory slope and PCCE will be evaluated for each project. The research will focus primarily on validating the effectiveness of the existing laboratory compaction effort in the State of Iowa; the theory or assumption of overcompaction in the laboratory leading to undercompaction in the field will be validated in this study. The experimental plan is described in detail in Chapter 3.

Significance of Work

The study will provide a better understanding on the overall effect of the existing N_{design} used in Iowa. The outcome of the project will greatly impact the designs of future flexible pavements and will widely be implemented once validated.

Organization

The following thesis is divided into five chapters, Chapter 1, provides the introduction and background to the importance of compaction effort in HMA, problem statement, objectives, methods and approach and significance of work. Chapter 2 is the literature review which presents the previous studies conducted on validating N_{design}. Chapter 3 describes in detail the experimental plan and testing methods used in this study. Chapter 4 presents the overall results and analysis. Chapter 5 summarizes the conclusions, recommendations and provides future research in regards to identifying an optimum N_{design} for the State of Iowa.

CHAPTER 2: LITERATURE REVIEW

History of Asphalt Mix Design

Early asphalt mixtures were primarily based on empirical design analysis (i.e., selecting optimum asphalt content). Industries/agencies relied heavily on precedent experience to evaluate and determine the appropriate mix type for selected projects at different locations with varying temperatures. A good and bad mix would be differentiated based on the pavement performance of the existing pavement structure and the mechanics of the asphalt material were not taken into consideration. The use of hot mix asphalt (HMA) concrete significantly increased throughout the years and the need for standardized testing was essential to the design process [6]. Overtime, the use of empirical design was insufficient due to factors/variables varying significantly with time. In the 1920s, the most popular early asphalt mix design method was the Hubbard-Field mix design [5]. The Hubbard-Field method later influenced the Marshall and Hveem methods during the 1940s through the 1960s. In 1987, the SHRP began developing the Superior Performing Asphalt Pavement System (Superpave) and by 2008, most states including the State of Iowa adopted the mix design method [4].

The importance of simulating field compaction in the laboratory became one of the primary concerns in the industry. Francis Hveem developed the Hveem mix design method in the mid-1920s for the State of California DOT and is designed primarily for the western states [5]. The method was developed to improve pavement performance with the use of the “oil mix” (combination of asphalt oil and aggregate) for low traffic volume highways in California [5]. He concluded that fine mixes required higher optimum asphalt content due to its larger surface area

and with this determined the appropriate amount of asphalt content from the particle size distribution or gradation [4]. The gradation in HMA is one of the most effective means in determining the effectiveness of the performance of aggregate materials as a pavement structure. Gradation is determined by passing aggregate materials through a series of stacked sieves known as sieve analysis [5]. Figure 1 is an example of gradation curves used in HMA design. Previous studies showed that the more asphalt content used on the aggregate particle, the thicker the film thickness and as a result improve pavement durability [7]. The strength (or stability) of the mix was tested using the Hveem stabilometer and the kneading compaction was used to simulate field compaction in the laboratory.

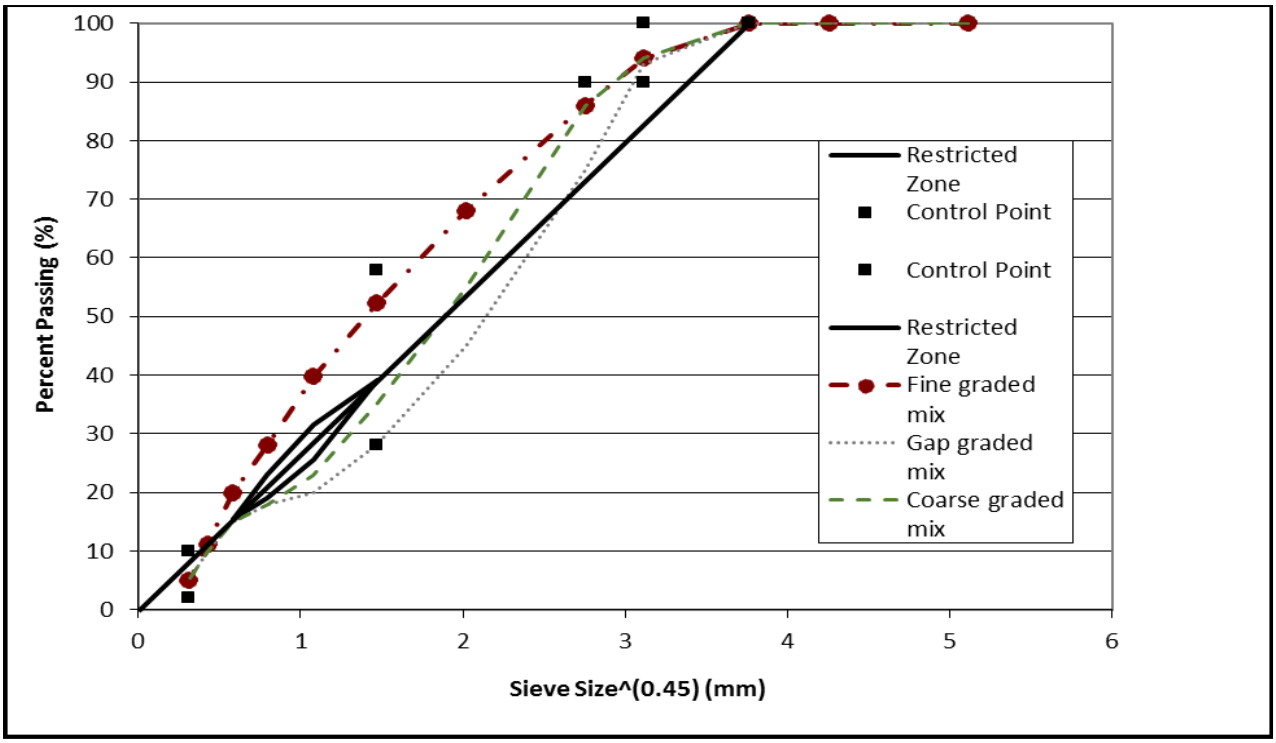

Figure 1: Typical Superpave mixes

Because other states were unable to use the Hveem mix design, in the late 1930s, the Marshall method introduced by Bruce Marshall was implemented. The Marshall method focused widely on the compaction effort of HMA and emphasized greatly on air voids. In the early 1990s, with the limitations of the early mix design methods, SHRP developed the Superpave mix design method [5]. The Superpave mix design method primarily focused on limiting/controlling detrimental pavement distresses. In order to do so, the mix design takes into account the changes in environmental conditions, traffic load and axle configurations. Additionally, Superpave evaluates the asphalt binder, aggregate properties/characteristics, mixture analysis and the material and volumetric (of compacted samples) properties in the HMA. The volumetrics was primarily used to determine the optimum asphalt content in the mixture. The compaction device used to compact laboratory specimens is known as the Superpave Gyratory Compactor (SGC), a compaction device similar to the French gyratory. The gyrations were heavily dependent on the traffic levels generally expressed as 18,000 lb. equivalent single axle load (ESAL). SHRP initially compacted samples at an angle of 1.0°, but later changed the internal angle of gyration to 1.16°, (external angle 1.25°) with a constant vertical pressure of 600 kPa [4]. Based on a study conducted by the National Cooperative Highway Research Program (NCHRP) project 9-9, different levels of compaction effort was recommended for Superpave and is denoted as $N_{initial}$, N_{design} and $N_{maximum}$ as shown in Table 1 [4].

Because Superpave was designed only to test for asphalt binder and volumetric properties of a mixture, agencies were hesitant to rely only on this and as a result many began using supplemental tests such as the Hamburg Wheel-Tracking Device and the Asphalt Pavement Analyzer [5]

Table 1: NCHRP Compaction Parameters [8]

Design ESALs (millions)	Compaction Parameter		
	$N_{initial}$	N_{design}	$N_{maximum}$
< 0.3	6	50	75
0.3 to < 3	7	75	115
3 to < 30	8	100	160
> 30	9	125	205

Comparison of the mix design methods

While the Hveem method is excellent in simulating field densities, the method is only developed primarily for the western part of the U.S. and is not recommended for use outside of that area. In addition, the kneading compaction device is expensive, not portable and thus is not widely implemented due to cost. Alternatively, the Marshall mix design method uses an inexpensive and simple compaction device. Both methods focused on the voids, strength, and durability of the mix [9]. Today, the Superpave mix design method is the most widely used method in flexible pavements design and analysis. In terms of compaction methods, the primary difference between Superpave and the Marshall and Hveem methods is the ability of the SGC device to monitor the change in height during the compaction process. See Figures 2 and 3 for compaction devices. While it is relatively simple to conclude that the evolution of mix design has

led to improved design practices, the validation of the gyratory levels, mainly the N_{design} table still requires further evaluation in terms of the effectiveness of compaction effort in the field.

Figure 2: HMA compaction device. Left: California kneading compactor. Middle: Marshall hammer. Right: Superpave Gyratory Compactor (FHWA)

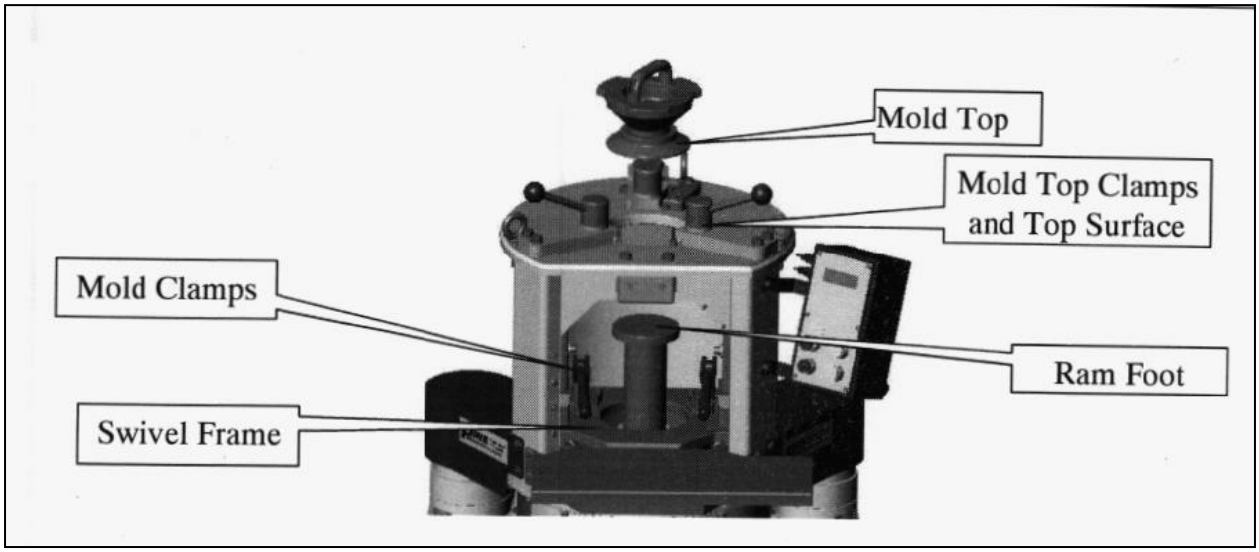

Figure 3: Pine Instrumental Company, AFG2AS/AFG2CS Superpave Gyratory Compactor. [1]

Superpave N_{design}

The significance of N_{design}

The N_{design} is known as the design number of gyrations or compaction effort used in Superpave HMA. To simulate field compaction in the laboratory, SHRP conducted numerous studies and extracted core samples from randomly selected projects. This allowed SHRP researchers to match in-place densities to a number of gyrations and as a result, generated the N_{design} table [4]. The ultimate purpose of conducting a laboratory test is to produce small-scale specimens and test for material characterization, volumetric properties and predict pavement performance/distresses of HMA. This allows researchers to produce the most cost-effective solution for industries/agencies and conduct a large-scale pavement test to further evaluate/validate the pavement performance tested in the laboratory. Standardized tests state that test specimens are compacted to a target air void of 4% (or 96% theoretical maximum density) using the design number of gyrations corresponding the appropriate traffic level. The theoretical maximum density of a mixture is the specific gravity of the HMA excluding air voids [5]. In the field, the asphalt concrete is initially compacted to 7% air voids and traffic loads are used overtime to further densify the pavement to its 4% target air voids [10]. NCHRP project 9-9 concluded that the ultimate pavement density was achieved 2 to 3 years post-construction. However, other studies monitored ultimate pavement densities to occur over an extended period of time [19]. The laboratory mix designs with a high level of SGC compaction effort has led to field mixtures that are difficult to place and compact to 7% air voids in the field. In addition, the pavement is not densified further so it will never reach the 4% target air voids. The relationship between the laboratory compaction effort and the field compaction does not provide a strong correlation. The levels of gyration is critical in design because overcompaction in the laboratory

design can lead to higher air voids in the field due to undercompaction during the compaction process, which consequently leads to durability issues in pavement [11]. Similarly, undercompaction in the field will cause higher ultimate pavement density which leads to bleeding or rutting [17]. A desirable, stiff asphalt mixture consists of a good aggregate skeleton and/or low asphalt content and generally compacts to 4% air voids after the pavement has been densified by traffic; whereas a weak asphalt mixture with the same compaction effort overcompacts to 2% air voids [12]. Note that the stress distribution of flexible pavements differ than concrete pavements, see Figure 4.

The laboratory compaction effort or N_{design} is important in the determination of the optimum asphalt content as well as approximating the ultimate pavement density in the field. The optimum asphalt content is critical in design because mixes that have excessive asphalt will undergo permanent deformation, while too little asphalt causes difficulty in field compaction which leads to early fatigue cracking (voids in mineral aggregate, VMA will subsequently be affected). Generally, achieving target pavement density and excellent construction quality are essential in producing a durable and long lasting pavement structure.

Figure 4: Stress distribution of flexible pavement [2]

Disadvantages/Issues

The optimum binder content is one of the most important design parameters in flexible pavement or HMA design. Several agencies claim that under the Superpave method, the asphalt binder content is reported to be too low and thus has been known to cause durability issues in the pavement [13]. Additionally, other agencies believed the existing N_{design} values were higher than required and consequently pavements were unable to achieve ultimate pavement density within 2 to 3 years post construction [14]. As a result, many states had conducted local studies to verify/validate the N_{design} values in the Superpave method.

Validation of N_{design}

NCHRP Report 573

The National Center for Asphalt Technology at Auburn University was assigned NCHRP Project 9-9, "Verification of Gyration Levels in the N_{design} Table"; the final report is the NCHRP Report 573 published in 2007. The primary goal of the project was to validate the current design gyration levels in the AASHTO Standard Practice R 35 for four 20-year design traffic levels at traffic volumes including the following: less than 0.3 million, 0.30 million to 3 million, 3 million to 30 million, and greater than 30 million ESALs) while monitoring field performance [4]. The research team studied 40 field projects in 16 states with different traffic volume levels, aggregate and gradation types and asphalt binder performance grades, see Figure 5 for locations. One out of 40 projects used a compaction effort of 50 gyrations, 12 projects used 75 (68-86), 18 projects used 100 (90-109) and 9 projects used 125 gyrations. In addition, 11 projects, 26 projects and 3 projects used a NMAS of 9.5 mm, 12.5 mm and 19.0 mm respectively. For each project location,

prior to construction, loose mix samples were taken from the asphalt plant and three specimens were replicated and compacted to 100 and 160 gyrations; a total of about 26 to 36 specimens per project were compacted.

Figure 5: Location of NCHRP Project 9-9 field studies [4]

Researchers extracted three cores along the right of the wheel path shortly after construction, 3 months, 6 months, 1 year, 2 years and 4 years post construction. Each project was monitored until the ultimate in-place density was achieved. The ultimate in-place density would then be matched with the N_{design} used in the initial mix design. The recorded average in-place density for the 40 projects was 91.6 percent of G_{mm}, where 55% of the projects showed densities below 92 percent of G_{mm} and 78% displayed densities less than 93 percent of G_{mm} [4]. Based on the results, about 63% of the pavement densification occurred in the first 3 months after construction. The densification showed little to no difference between 3 months and 6 months after construction. This occurred because projects completed in the summer would experience cooler temperature in the following months after construction, thus the change in densification from 3 months to after 6 months were insignificant. At 50-percent frequency the percent G_{mm}

between 6 months and 1 year increased by 0.8 (93.6 percent to 94.4 percent G_{mm}) and showed a slight increase of 0.2 percent between 1 year and 2 years. The project extended to monitor after 4 years post construction to ensure pavement reached ultimate in-place density. The recorded average in-place density for the 40 projects after 2 and 4 years was 94.6 percent of G_{mm}.

To verify, a test comparing the 2 year and 4 year in-place densities were conducted, where the null hypothesis tested that the average 2 year density was identical to the average 4 year density. The test concluded that there was no statistically significant difference in the 2 year and 4 year in-place densities. Thus, it is evident to conclude that pavement densification occurs after 2 years. However, numerous factors may contribute to pavement densification, such as performance binder grade, weather conditions, high oxidation, etc. Researchers conducted four different analyses to match the ultimate in-place density to the N_{design}. The following analyses were conducted: (1) regression of the predicted N_{design} and traffic volume after 2 years, (2) regression between ESAL levels at different time intervals and the predicted gyration matching in-place density at the corresponding time intervals, (3) models, and (4) ultimate in-place density related to N_{design}. Additionally, researchers attempted to use the concept of the locking point developed by Illinois DOT [4].

Gyratory Locking Point (LP)

The LP concept is considered an alternative to N_{design} and is created to prevent overcompaction and aggregate deterioration. It is assumed that during the compaction process, the aggregates in the mixture are damaged as the rollers continue to compact to its construction air voids. The concept was developed to prevent damage in the aggregates and instead provide

good aggregate interlock. Out of the four different locking points tested, only 3-2-2 showed the best relationship to the 2 year in-place densities, but the results were weaker compared to the design traffic, see Figure 6 [4]. As a result, this approach was no longer evaluated based on the findings.

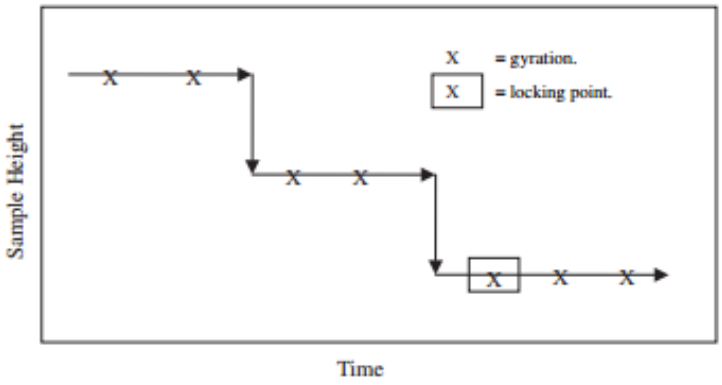

Figure 6: Illinois 3-2-2 locking point [4]

$N_{initial}$ and $N_{maximum}$

Initially, Superpave produced three levels of gyrations for each traffic level, N_{inital}, N_{design} and N_{maxium}. The air voids were measured based on the three levels to determine the quality of the mixture [5]. The specification states that air voids should meet a minimum value at N_{ini}, 11% air voids at N_{design} and 2% air voids at N_{max}. The use of N_{ini} in design is to guarantee the HMA mixture is not too soft or tender during the compaction process and in addition ensure rutting resistance [15]. Similarly, N_{max} is used in design to validate rutting resistance. The N_{ini} and N_{max} for the 40 projects were also evaluated. It was recorded that 11 out of 40 projects had at least one sample that failed N_{ini} and 25 of 40 projects had at least one sample failed N_{max}. The research team concluded based on the results obtained from study that the current N_{design} levels used in

AASHTO R 35 were significantly higher than the ultimate pavement density, primarily at ESAL levels greater than 0.3 million. Figure 7 displays the general concept of N_{design}.

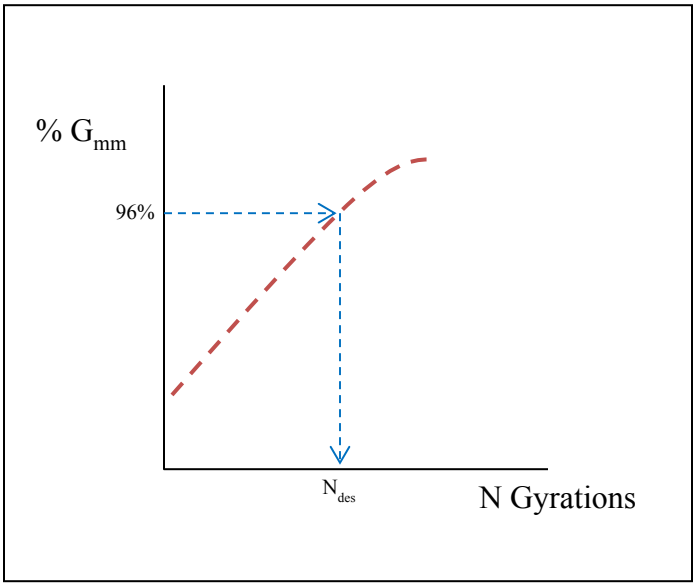

Figure 7: Concept of N_{design}

NCHRP Recommendations

The research team presented the following recommendations: (1) reduction of the existing N_{design} Table primarily for mixes designed with modified asphalt binder with a performance grade of PG76-XX or greater, (2) Removal of $N_{initial}$ and N_{max} in existing N_{design} Table, (3) Specification for the angle of gyration revised to a dynamic internal angle (DIA) of 1.16°± 2° and (4) Option to consider the N_{design} at the 2-year design traffic volume. Table 2 summarized the final recommendation as a result of validating the N_{design} for NCHRP Project 9-9 [4].

Table 2: NCHRP Recommended Ndesign Levels for SGC DIA of 1.16° ± 2 [4].

20-Year Design Traffic, ESALs	2-Year Design Traffic, ESALs	N_{design} for binders < PG 76-XX	N_{design} for binder PG 76-XX or mixes placed > 100 mm from surface
< 300,000	< 30,000	50	NA
300,000 to 3,000,000	30,000 to 230,000	65	50
3,000,000 to 10,000,000	230,000 to 925,000	80	65
10,000,000 to 30,000,000	925,000 to 2,500,000	80	65
> 30,000,000	> 2,500,00	100	80

Reduction of N_{design} in other States

It was evident based on pavement surveys collected that Superpave mixes performed significantly well against rutting due to lower binder contents used. However, researchers observed that many pavements experienced early fatigue cracking [16]. Fatigue or alligator cracking is a form of pavement distress generally caused by fatigue failure on the HMA surface under repeated loading [5]. Fatigue cracking can be due to an increase in loading, inadequate compaction and structural design, stripping, and possible loss of support of base, subbase and/or subgrade layers [5]. Additionally, NCHRP Report 573 concluded that mixes with higher gyration levels provided better rut resistance, but may lack sufficient durability [4]. As a result, many states conducted various tests to verify the existing design number of gyrations and evaluated the

effect on pavement performance. Such states include Colorado, Georgia, Virginia, Ohio and so forth. The primary focus of each study is to validate the in-place design number of gyrations of HMA in each state over a span of 5 to 6 years depending on the project specification.

The Colorado Department of Transportation (CDOT) found that none of the pavements randomly selected reached the design air voids after 6 years. The average in-place field voids for years 3, 4, 5 and 6 years displayed a difference of 1.2% air voids at Superpave N_{design} between the line of equality at 4% air voids, see Figure 8 for visual interpretation [3]. In this case, the line of equality is used for comparing the percent air voids at Superpave N_{design} with the percent air voids at a specific year. In Figure 8, the average in-place field voids at 3 years show that there is a difference of 1.2% air voids between the two parameters. The results indicate that the field air voids are undercompacted and thus the current design number of gyrations being used was too high. CDOT determined that a reduction of 30 gyrations is required in order to match the in-place ultimate pavement densities. However, such a reduction was not desired for CDOT. The pavement performance was also evaluated throughout the study; low to moderate rutting was detected but no major distresses were observed. The final recommendations of CDOT concluded 75 gyrations were used for lower traffic levels and 100 gyrations for higher traffic levels. In Georgia Department of Transportation (GDOT), the average in-place air voids after 5 years were 5.7%. GDOT concluded that 66 gyrations matched the in-place densities in Georgia and thus selected a design number of gyration of 65 for Superpave mixes (performance grade should be adjusted according to the traffic level) [17]. Ohio Department of Transportation (ODOT) specified the design number of gyration to about 65 based on the annual daily truck traffic (AADT) [18]. In the State of Virginia, Virginia Department of Transportation's (VDOT) primary

concern was slightly different than simply verifying N_{design} levels [13]. VDOT's concern is that the existing Superpave mixes do not have sufficient asphalt content, thus reducing the pavement life and serviceability [11]. The primary goal is to provide better pavement serviceability while controlling rutting or bleeding in the pavements in Virginia. Virginia has lowered the number of gyrations since using the Superpave mix design method in order to accommodate for the low asphalt content. The lower gyration levels required an increase in asphalt content and as a result increased the overall durability of the pavement [13].

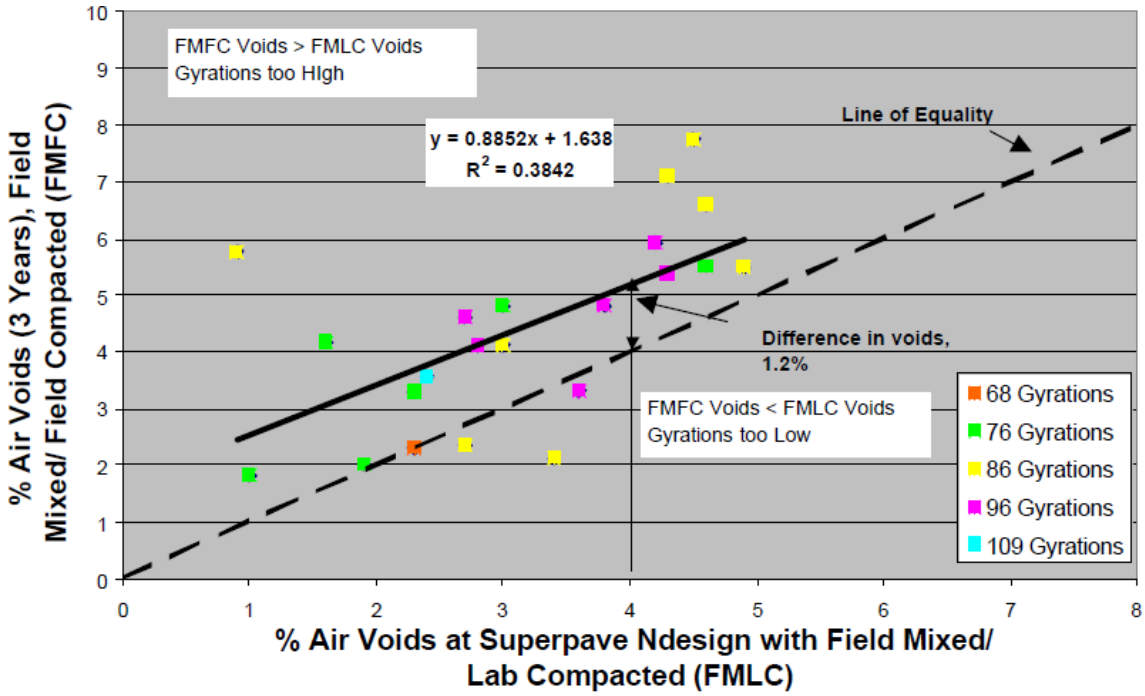

Figure 8: FMLC versus FMFC Air Voids after 3 Years [3]

Effects on Pavement Performance

To design an adequate flexible pavement structure, the three principle pavement distresses considered in design are fatigue cracking, rutting and low temperature cracking.

Rutting

Rutting occurs due to an accumulation of permanent deformation along the wheelpaths caused by excessive traffic loading (rut depth) and/or high temperature; and as a result causes compressive strain at the top of each layer, see Figure 9. Rutting can also occur due to inadequate compaction during construction [5]. The severity level can be detected by following the *Highway Pavement Distress Identification Manual for LTPP*. High severity rutting, if left untreated can lead to hydroplaning caused by the build-up of water and therefore may lead to structural failures [11]. Additionally, excessive rutting can cause serviceability issues because the ride quality becomes inadequate for travelers [5]. About 32% of rutting occurs in the surface layer and 14% and 45% in the base and subbase respectively [11]. Generally, with the existing N_{design} used in Superpave, rutting resistance has not been reported to cause major inadequacies to the pavement structure. Thus, reducing the N_{design} value can negatively affect the rutting resistance and consequently increase permanent deformation in the structure due to higher asphalt content [15].

Figure 9: Severe rutting in flexible pavement [19]

The most common problem with conducting pavement performance testing is the cost of the test devices. NCHRP Report 478 conducted a study to determine the relationship of SGC properties to HMA rutting behavior. It has been believed that there is a relationship between the compaction slope of the SGC and the rutting behavior of HMA. Based on a previous study involving Watsonville Granite, the results showed that for higher compaction slope mixture, the shear stiffness was higher but the permanent shear strain was lower [12]. According to NCHRP Report 478, "the main problem in relating compaction slope to mixture performance properties is that the compaction slope, unlike mixture performance, is not sensitive to asphalt binder content" [12]. Researchers involved in the study developed a compaction parameter to correlate the SGC to the rutting performance of an asphalt mixture. However, further research is needed to validate the compaction parameter determined in this study. Meanwhile, tests such as the Hamburg Wheel-Tracking Device and the Asphalt Pavement Analyzer may be used to test for rutting resistance [4].

Fatigue Cracking

Fatigue cracking in flexible pavements causes horizontal tensile strain at the bottom of the asphalt or base layer under repeated traffic loading, see Figure 10(a). The small cracks start at the bottom of the asphalt or base layer and propagate to the surface layer resulting in a series of interconnecting cracks caused by fatigue failure [11]. There are many factors that contribute to fatigue cracking, such as improper design (QC/QA), pavement material characteristics, weak subgrade soil, traffic loading, moisture due to poor drainage and temperature. While too much

binder causes bleeding in pavements, too little can cause fatigue cracking because the pavement is unable to flex or bend to accommodate traffic load and/or temperature changes [11].

If left untreated excessive fatigue cracking will result in loose surface materials that will ultimately lead to potholes, as shown in Figure 10(b). Pavement rehabilitation is required in order to restore pavement conditions and increase serviceability. However, the underlying pavement layers in addition to the traffic loads must be evaluated and considered in design prior to the rehabilitation process because weak layers do not provide sufficient support to accommodate or withstand traffic loads [5]. Previous studies have shown that mix design using Superpave showed early signs of fatigue cracking. In order to reduce the fatigue cracking, different agencies suggested adding enough binder to reduce/delay cracking.

Figure 10: Fatigue cracking (left). Pothole caused by fatigue cracking (right) [20]

Thermal Cracking

Thermal cracking is similar to fatigue cracking and is caused by repeated loads, in addition temperature changes [11]. There are two types of distresses under this category, low-temperature cracking and thermal fatigue cracking. Low-temperature cracking occurs primarily in the northern part of the United States where temperatures drop below -10°F, whereas thermal fatigue cracking occurs in locations with moderate temperature where the asphalt becomes too oxidized [11].

To reduce/delay thermal cracking, the proper asphalt binder type used for locations with low temperatures must be used. Additionally, the asphalt binder should not be overheated during construction because the binder oxidizes and stiffens. Hornbeck suggested that increasing the film thickness may also assist in preventing thermal cracking [14].

Figure 11: Block cracking, type of thermal cracking [21]

CHAPTER 3: EXPERIMENTAL PLAN AND TESTING METHODS

Introduction and Overview

The study will evaluate the concerns with the use of the nationally recommended N_{design} levels in the State of Iowa and identify the problematic ESAL levels. The outcome of the study will determine how the current N_{design} levels affect the overall pavement density.

This research will focus primarily on field sections; see Figure 12 for the flow chart visualization on the experimental plan. The evaluation of existing pavement conditions will be closely examined using the Pavement Management Information Systems (PMIS) surveys and the Highway Pavement Distress Identification Manual for the Long-Term Pavement Performance Program (LTPP). Identification of field pavements throughout Iowa was randomly selected with the assistance of Iowa Department of Transportation (DOT). Based on the availability of pavement condition data, eight projects were selected to evaluate existing pavement conditions. Field density measurements were collected and compared to QC/QA data to ensure quality in design and construction. Additionally, the gyratory slope and the post-construction compaction effort (PCCE) was calculated and evaluated in the study. The theory of overcompaction in the laboratory leading to undercompaction in the field will be validated. A he following diagram in Figure 12 summarizes the experimental plan for the study.

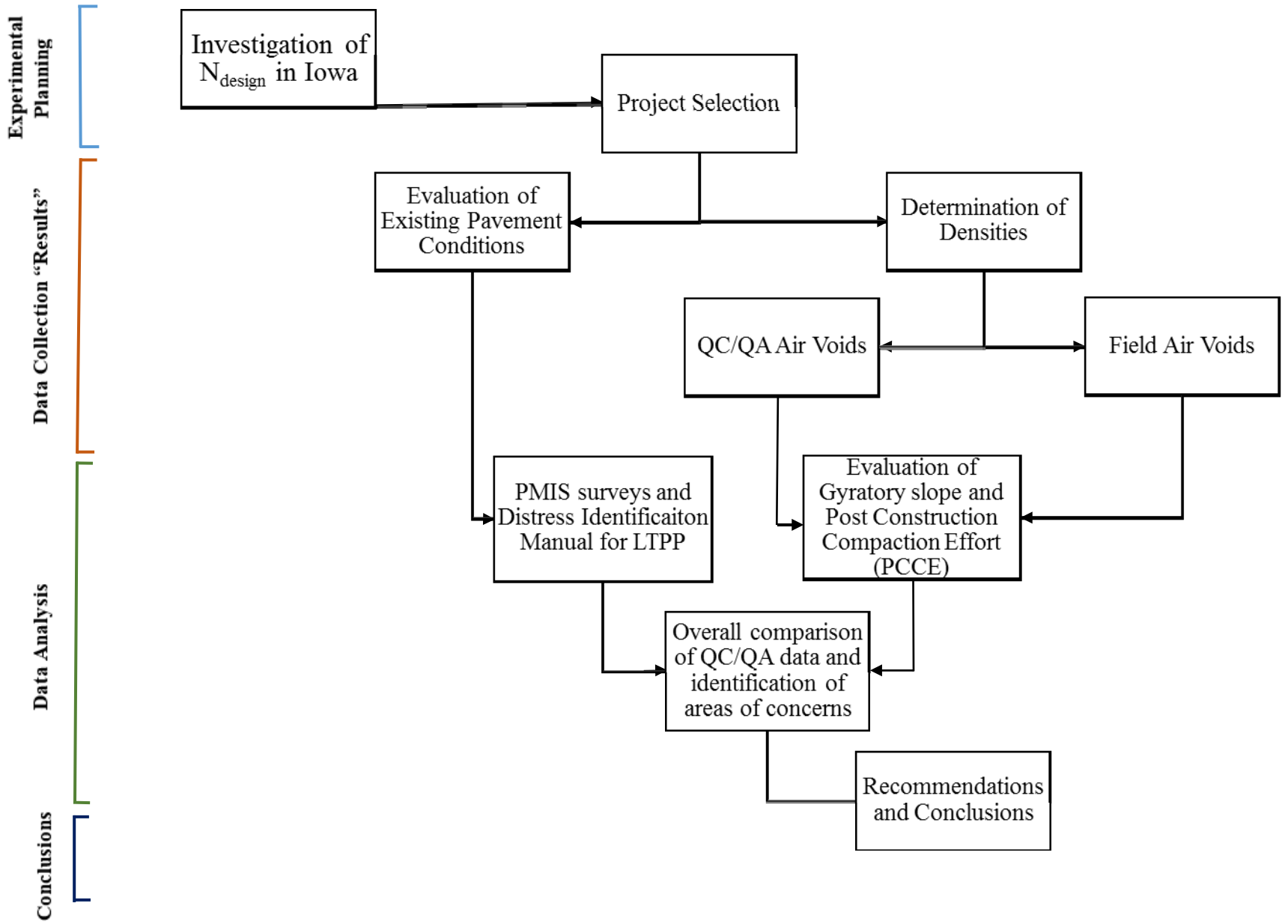

Figure 12: Flow chart of experimental plan for the study

Project Selection

Three asphalt pavement projects for each ESAL category from the 2011 construction season were randomly selected throughout the State of Iowa to evaluate the design number of gyrations and to validate whether or not ultimate pavement density has been achieved. Projects selected varied in traffic levels ranging from 100K to 10M ESALs, as well as the compaction effort or N_{design}. The project details such as the average annual daily traffic (AADT) are shown in Table 3 and locations for each project are displayed in Figure 13. Additional project information is located in Appendix A. Three projects per ESAL level category were selected and within the projects, three specified milepost locations were randomly chosen for field coring/testing. The Iowa IDOT assisted in the removal of three 4" field cores along the wheel path at each milepost, four years post-construction. Only the surface mixes were used to evaluate densification due to traffic loads.

The ESAL levels selected for the experimental plan are representative of more than 90% of the mixes that were constructed in the State of Iowa for 2011 construction season. The cumulative distribution of surface mixtures constructed in 2011 is presented in Figure 14. In Figure 14, a small distribution of the projects selected was approximately 14% at 100-300K ESALs. Traffic levels ranging from 1M to 3M constitutes about 65% of the asphalt pavements constructed in 2011.

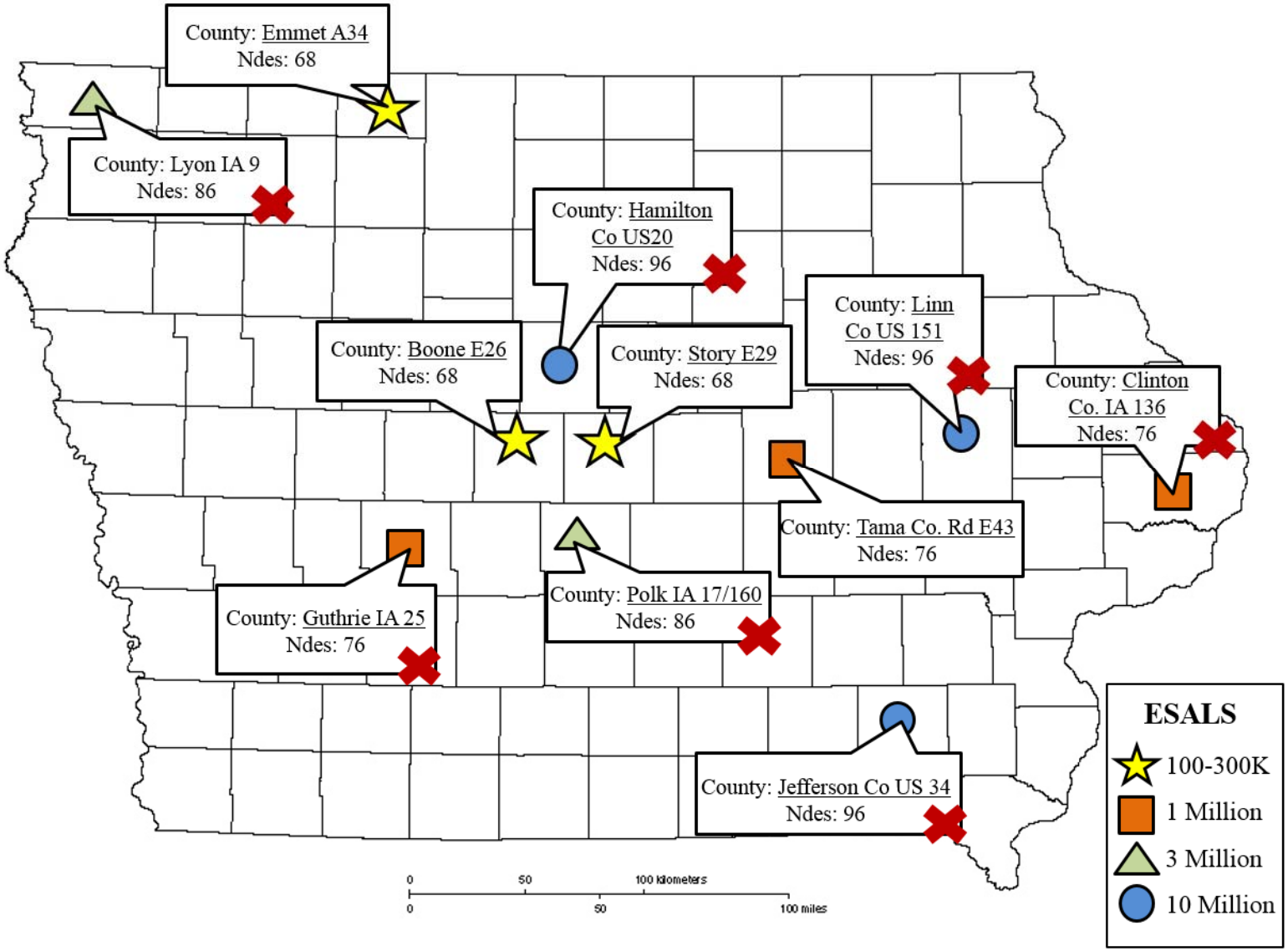

Figure 13: Identification of field sections in Iowa, specific project locations in Iowa

Table 3: Project location for the study

Project No.	Project Location	Mile Post	AADT	ESAL Level	N_{des}
1	Boone E26	0.59	690	100-300K	68
		0.77	690		
		1.26	690		
2	Emmit A34	0.46	320		
		1.16	320		
		1.64	730		
3	Story E29	0.18	560		
		0.4	560		
		1.91	560		
4	Clinton Co IA 136	4.5	1230	1M	76
		5.9	1230		
		13.6	2110		
5	Guthrie County IA 25 MI	78.1	1100		
		80.31	1100		
		83.05	1100		
6	Tama County Co Rd E43	1.43	740		
		5.42	740		
		7	740		
7	Polk IA17	7.99	980	3M	86
		9.83	980		
		11.84	980		
8	Polk Co IA 160	0.16	21600		
		0.28	21600		
		0.51	21600		
9	Lyon Co IA 9	1.73	3290		
		1.74	3290		
		3.66	3290		
10	Linn Co US 151	31.42	7300	10M	96
		32.93	7300		
		33.03	7300		
11	Jefferson Co US 34	204.38	5200		
		216.97	5200		
		217.78	5200		
12	Hamilton Co US20	136.22	8200		
		136.38	8200		
		137.07	8200		

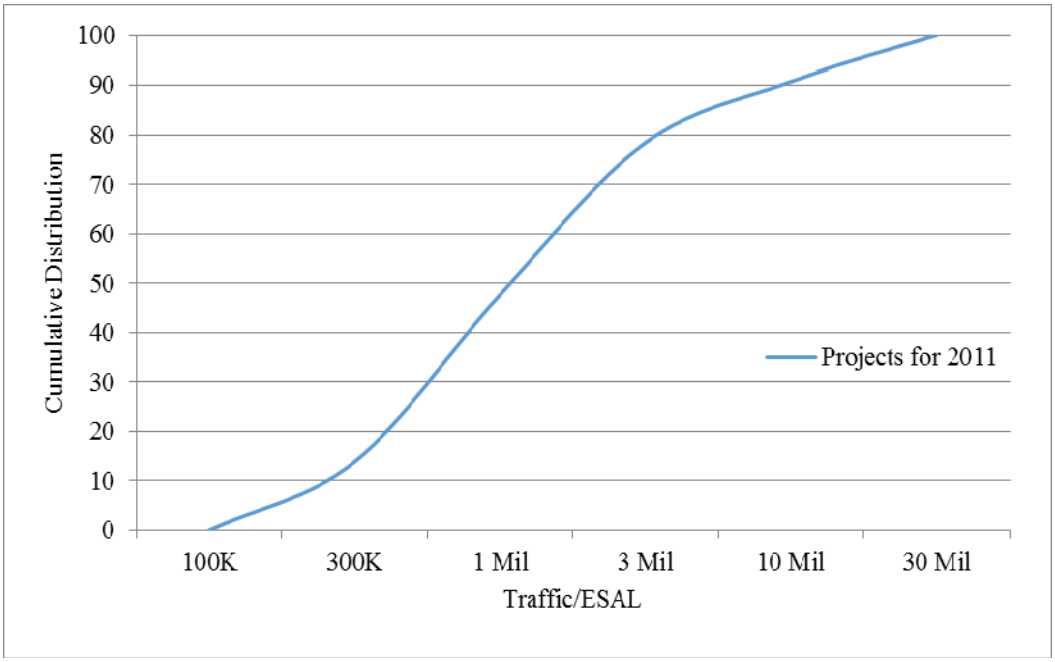

Figure 14: Cumulative distribution of surface mixes

Evaluation of Existing Pavement Conditions

Flexible Pavement Distresses

Distresses in a flexible pavement structure are an important consideration in design because it is an initial indication of pavement failure. According to the *Highway Pavement Distress Identification Manual for LTPP,* the main structural pavement distresses in flexible pavements are fatigue cracking, block cracking, edge cracking, longitudinal cracking (wheel path/non-wheel path), reflection cracking at joints and transverse cracking [22]. In addition to the structural distresses, functional distresses such as the International Roughness Index (IRI) was also examined. There are three levels of severity for each type of distress: low, moderate and high. In accordance to the *Highway Pavement Distress Identification Manual for LTPP,* Table 4 provides a brief description of each severity level corresponding the type of distress. In short, a suitable functional pavement performance yields low IRI, high present serviceability rating

(PSR), high skid number (SN), and minimum transverse, longitudinal and fatigue cracking; note that all distresses are due to tensile strain or stress in the asphalt concrete (AC) layer.

Table 4: Level of severity corresponding type of distress [22]

Type	Severity Levels
Fatigue	**Low:** A small percentage of cracks present; not spalled or sealed.
	Moderate: An initial formation of interconnecting cracks developing into a pattern; somewhat spalled; possible cracks sealed
	High: Moderate to high interconnected cracks formed complete pattern; severely spalled; possible cracks sealed; possible pumping present.
Transverse	**Low:** Unsealed crack with a mean width of 6 mm or less; a decent condition sealed crack with sealant material, mean width unable to determine.
	Moderate: Any cracks with a mean width greater than 6 mm but less than or equal to 19 mm; or any cracks adjacent to low severity with a mean width of 19 mm or less.
	High: Any cracks with a mean width greater than 19 mm; or any cracks adjacent to moderate to high severity with a mean width of 19 mm or less.
Longitudinal	**Low:** Unsealed crack with a mean width of 6 mm or less; a decent condition sealed crack with sealant material, mean width unable to determine.
	Moderate: Any cracks with a mean width greater than 6 mm but less than or equal to 19 mm; or any cracks adjacent to low severity with a mean width of 19 mm or less.
	High: Any cracks with a mean width greater than 19 mm; or any cracks adjacent to moderate to high severity with a mean width of 19 mm or less.
Patch/Patch deterioration	**Low:** patch has low severity distress (rutting < 6 mm); pumping is not present.
	Moderate: patch has moderate severity distress (rutting < 6 mm to 12 mm); pumping not present.
	High: patch has high severity distress (rutting > 12 mm); or additional patch material within original patch; pumping present.

Selection and determination of pavement condition using PMIS

In pavement design and analysis, the primary purpose of pavement engineers is to construct a pavement structure that is able to support traffic/environmental loads while providing users with a safe, comfortable and efficient mode of transportation. The performance and serviceability of pavements are ways to evaluate the condition of the structure. Pavement performance reflects condition changes or any structural inadequacies in the pavement structure to accommodate traffic volume over time whereas serviceability is the ability of the pavement system to serve traffic throughout the pavement life cycle [11].

Distresses in pavements negatively impact performance if left untreated and contribute to the deterioration and subsequent loss in structural integrity. The PMIS surveys are useful in primarily evaluating of the overall condition of the pavement and can additionally be used to recommend an appropriate rehabilitation/maintenance strategy for a given pavement section based on collected distress data. Graphical visualization of the severity of distresses before and after rehabilitation was generated to show if pavement conditions improved after rehabilitation.

Selected projects were categorized into its corresponding ESAL level and the severity levels when applicable, are shown in the graphs. Within the selected projects, eight projects were selected based on the availability of pavement condition data and was evaluated using the PMIS surveys. The PMIS data will demonstrate the severity in distresses induced on the pavement structure prior to rehabilitation. The selected projects chosen are shown in Figure 13, denoted with an “X”. Pre and post-construction field performance was analyzed based on LTPP manual classifications. Post-construction performance was compared with material characteristics of

field cores and QC/QA collected at construction. The QC/QA provided by the Iowa DOT presented design parameters such as the bulk specific gravity (G_{mb}) and theoretical maximum specific gravity (G_{mm}) of the mixture at construction both tested by the contractor and Iowa DOT, in addition to intended thickness and actual thickness of the HMA. The pavement performance data contained both the following structural and functional distresses: rutting, fatigue or alligator cracking, transverse cracking, longitudinal cracking and International Roughness Index (IRI).

Table 5 displays the county and ESAL levels for the projects that had accessible State network PMIS data. Pavement condition surveys were used to compare the pavement performance in low, moderate and high traffic volumes or specifically 1, 3 and 10 million ESALs. The N_{design} for each ESAL category varied; the higher the traffic volume, the greater the value for N_{design}. The results will identify which ESAL level(s) require further monitoring/evaluation.

Table 5: Project selected to evaluate pavement condition

Project No.	County	ESALS
4	Clinton	1 Million
5	Guthrie	1 Million
7	Polk	3 Million
8	Polk	3 Million
9	Lyon	3 Million
10	Linn	10 Million
11	Jefferson	10 Million
12	Hamilton	10 Million

Determination of Field Densities

Field cores were collected four years post-construction in June and July of 2015. The surface mixture from the field cores was isolated for testing by sawing off the appropriate thickness, as shown in Figure 15, refer to Appendix A – E for detailed QC/QA data. The field core densities were then compared to densities at construction obtained from the mix data.

The bulk specific gravity of the mix (G_{mb}) of the field specimen was determined in accordance to ASTM D6752/D6752M and AASHTO T166-13. There are two methods to measure the bulk specific gravity of a mixture, one is by using the corelock device, a vacuum chamber and the water tank and second is using the conventional method, which primarily uses only the water tank. The corelock method requires vacuum sealing bags and different sizes correlate to a different bag volume correction factor to determine the air voids. Dry weights are obtained prior to and after sealing as well as the submerged and dry weights after submersion. The volume of the sample is determined and the bulk specific gravity can then be calculated [23].

Figure 15: Actual field core samples

The corelock method is known to produce more accurate results for the specific gravity of the field and laboratory specimens. The concern of excess water absorption as well as water draining rapidly when samples are removed from the water tank cause problems with measurements and thus does not produce accurate results. Both methods were used in the determination of the bulk specific gravity of the field cores.

The first half of the samples was tested using the corelock method. The results of the corelock method did not have a significant difference in the bulk specific gravity in comparison to the conventional method. Thus, the remaining samples were tested using the conventional method. Using the conventional method, the dry, submerged and saturated surface dry (SSD) weights were obtained to calculate the bulk specific gravity. The SSD is defined as the condition when the external surface is "dry" but the internal part of the sample is saturated. The SSD weight obtained by patting the entire sample with a rag or towel [23].

Figure 16: Corelock method

Figure 17: Water bath used for conventional method

The theoretical maximum density (G_{mm}) was initially estimated per project milepost based on the closest stationing from the G_{mm} measured from the QC/QA hotbox of loose mix recorded by the Iowa DOT at construction. The actual G_{mm} for each core sample was then verified in accordance to AASHTO T 209. Two methods in AASHTO T 209 were used to determine the G_{mm} in the laboratory; the flask and metal bucket methods, as shown in Figure 18. The surface mix samples was heated in the oven at 105 ± 5°C for 30 minutes or until the core is tender enough to break apart. For the flask method, a total of 2000 grams of sample was tested [24]. Similar to the bulk specific gravity, the flask method is known to produce accurate values for G_{mm}. Both methods yielded the same results.

Figure 18: Metal bucket method (left) and flask method (right)

Evaluation of the Gyratory Slope and Post-Construction Compaction effort (PCCE)

As previously stated, the NCHRP 9-16 project was introduced to determine if there is a relationship between the gyratory compaction parameters, particularly the gyratory slope and the rutting behavior of a mixture. The findings showed that the number of gyrations at maximum shear stress could be related to the stiffness and rutting of a mixture. However, additional research was recommended. While no definitive conclusion can be drawn relating compaction slope to rutting from the report, evaluation of the slope may still provide valuable information in relation to the study [12].

In this research, mix design information was provided and the compaction slope was calculated from $N_{initial}$ to N_{design}. From this, the post-construction compaction effort (PCCE), as shown in Figure 19, which is the difference in theoretical N_{design} four years post-construction and at construction due to traffic was determined. The theoretical N_{design} four years post-construction

and N_{design} at construction is calculated by using the compaction slope equation presented in SHRP A-407 report, see equation 1. The average for each ESAL category was computed and is taken as the PCCE for that specific ESAL level.

$$Compaction\ slope = 100* [(C_{des} - C_{ini})/(log(N_{des}) - log(N_{ini}))]$$

Equation 1: SHRP A-407 compaction slope [12]

Where C_{des} = levels of compaction obtained at N_{design}

C_{ini} = levels of compaction obtained at N_{inital}

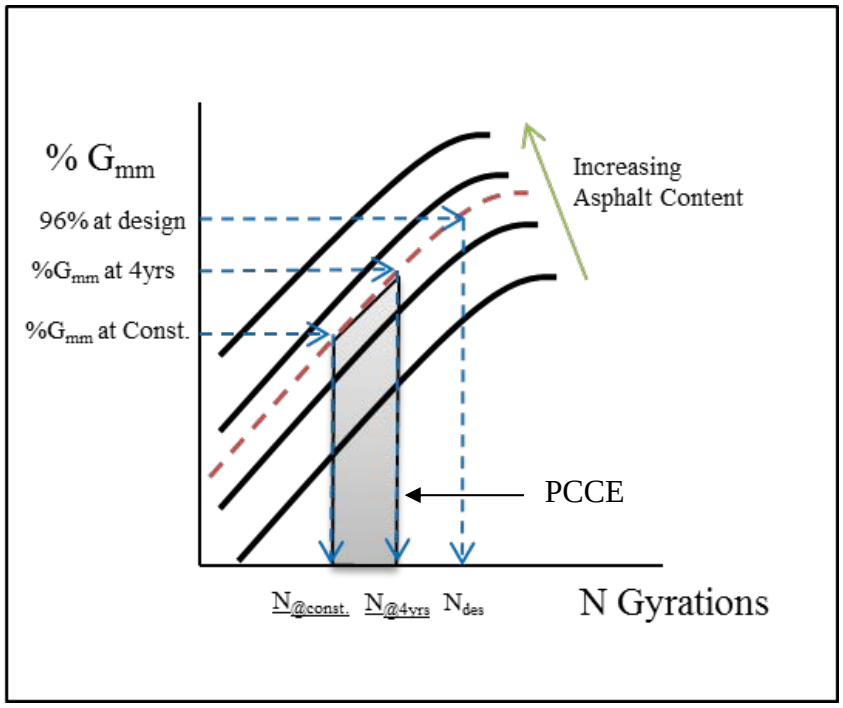

Figure 19: Conceptual representation of theoretical post-construction compaction effort (PCCE)

CHAPTER 4: RESULTS AND ANALYSES

Pavement Performance Evaluation using PMIS and LTPP

The Pavement Management Information System (PMIS) surveys were useful in evaluating the condition of the pavement structure prior to being overlaid. The state-owned roadways were selected because the PMIS data was readily available. The primary purpose of evaluating the PMIS data was to identify external factors that may impact the analysis. The projects were categorized into corresponding ESAL levels and the pavement distresses were categorized by type and severity levels when applicable. Figures 20 to 22 display a distress for each project with time in years on the x-axis and the corresponding pavement distress on the y-axis. The negative years represent time prior to rehabilitation while positive years indicate observations post-rehabilitation. The year "zero" represents 2011, the year of construction. The 2011 pavement distress surveys appear to have taken place both before and after reconstruction, depending on the project. The lines shown in Figures 20 to 22 represent the mean distresses for the corresponding severity level (if applicable); higher values represent more severe distress levels in the pavement structure.

The international roughness index (IRI) was selected as an overall indicator of ride quality and is shown in Figure 23. According to Iowa Interstate Corridor Plan IDOT, the following IRI criteria was developed: IRI < 95 indicates good pavement condition, IRI between 95 and 170 suggest fair condition, and if IRI is greater than 170 the condition is poor [25]. For the selected projects, the pavement with the historically highest IRI was 1M ESAL located in Clinton County, but all pavements showed significant improvement after rehabilitation. In

addition to the roughness index, other distresses such as transverse cracking, longitudinal cracking and rutting was investigated.

1 Million ESALS

Pavement conditions for projects 4 and 5 are displayed in Figure 20 where project 4 is shown in the upper portion of the graphs. Fatigue cracking for project 4, in Figure 20(a), indicate minor high severity cracking, whereas moderate cracking displayed a sharp drop in distress after pavement rehabilitation. Project 4, showed no sign of high severity fatigue cracking, but displayed a significant increase in moderate cracking two years prior to rehabilitation and subsequently improved thereafter. In Figure 23, project 5 showed fair IRI roughness levels and project 4 indicated a poor IRI condition prior to rehabilitation according to the criteria in Iowa DOT. Although the average IRI value for project 4 showed a slight increase two years after rehabilitation, the results still indicate good pavement condition.

The longitudinal cracking for projects 4 and 5 is shown in Figure 20(c). High and moderate longitudinal cracking was not as much of a concern as the low longitudinal cracking for project 5. The maximum average low and moderate cracking in project 5 both displayed an increase in distress at construction year until the year prior to rehabilitation; longitudinal cracking improved significantly after treatment. . In project 4, low severity cracking reached a peak in distress four years prior to rehabilitation while the moderate and high cracking stabilized the same year and remained constant. Transverse cracking shown in Figure 20(b), displayed similar trends to longitudinal cracking; low distress values in high severity cracking and high distress values for low severity cracking for both projects. The maximum low severity transverse

cracking in project 4 was nearly double the maximum low severity longitudinal cracking. There were small amounts of rutting recorded for both projects.

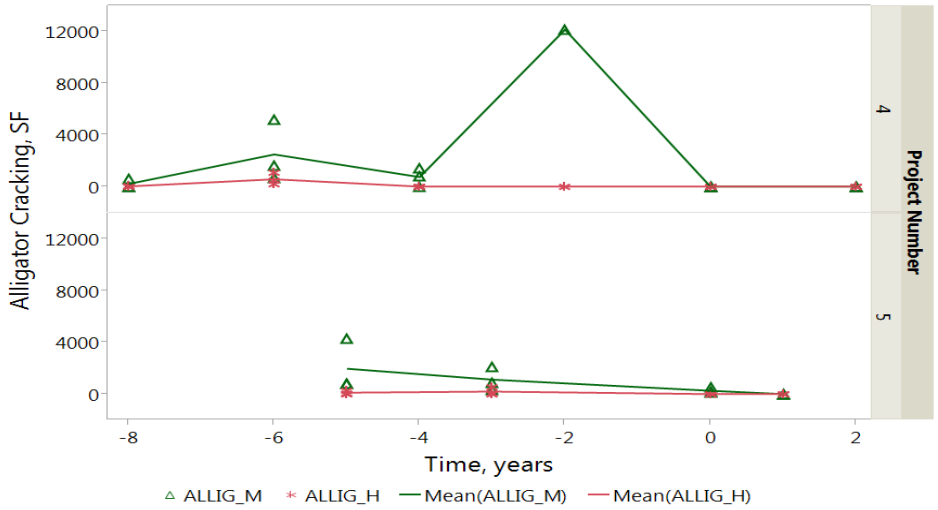

(a)

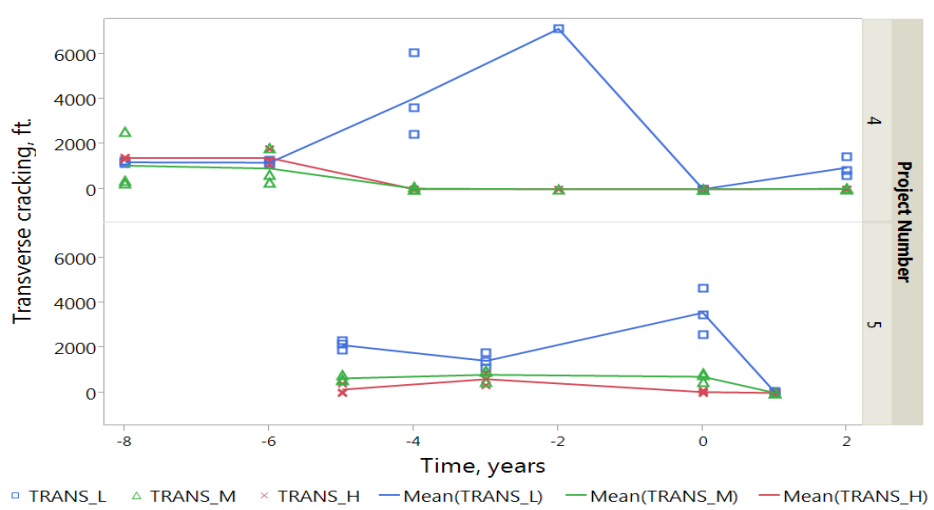

(b)

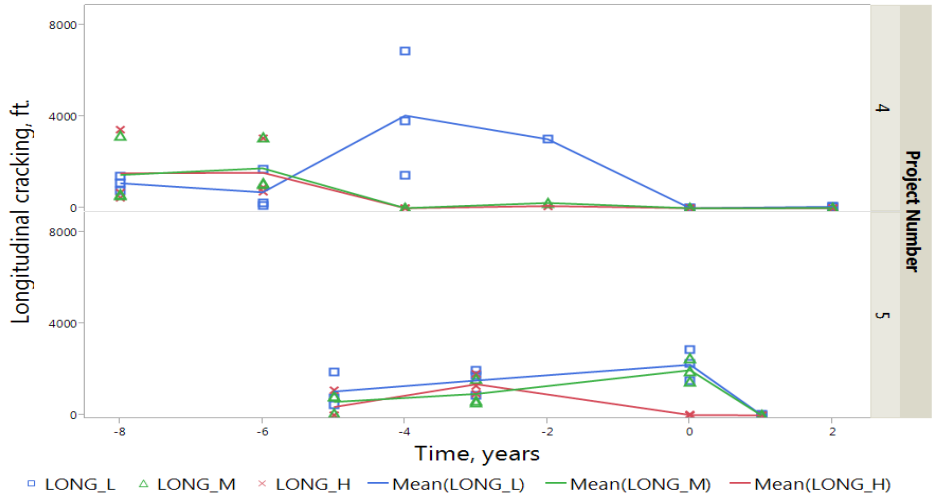

(c)

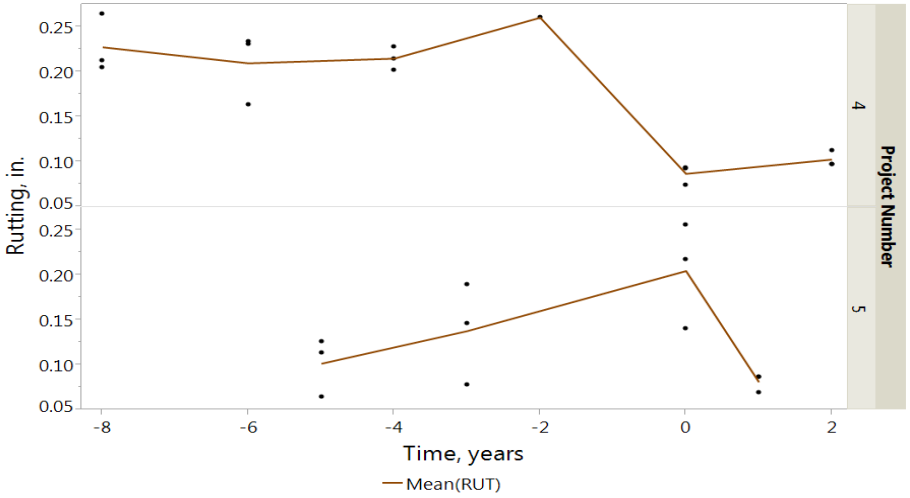

(d)

Figure 20: At 1M ESALs. (a) Alligator or Fatigue cracking, (b) Transverse cracking, (c) Longitudinal cracking, (d) Rutting

3 Million ESALs

Pavement conditions for projects 7, 8, and 9 can be viewed in Figure 21 (Project 7: top, Project 8: middle, Project 9: bottom). Project 8 has the least (or none) distress in pavements. Large amounts of patching were evident in project 8, specifically four years prior to rehabilitation. However, no conclusion can be drawn to relate the low pavement distress and the large patching conducted on the pavement section. Due to the findings in project 8, the following discussion will focus on projects 7 and 9. In all three projects, the average high severity fatigue cracking in Figure 21(a) remained constant at zero, while the average moderate fatigue cracking for projects 7 and 9 fluctuated throughout the recorded years. Project 7 displayed an average of 1000 square feet in moderate fatigue cracking prior to rehabilitation with post construction observations indicating no fatigue cracking. Project 8 IRI, shown in bottom of Figure 23, remained consistent and stable throughout the years examined. Based on IRI, the graphs indicate fair pavement conditions.

The pavements showed post-rehabilitation improvement in majority of the pavement distresses except for low severity transverse cracking in project 8 and rutting in project 9. In Figure 21(b), the low severity transverse cracking for project 8 had a slight increase in distress, but the effect may be negligible. The average rutting depth for all three projects shown in Figure 21(d) did not exceed 0.26 inches. The average IRI values after rehabilitation indicated good pavement conditions in all three projects and similar to one million ESALs, low severity longitudinal and transverse cracking produced the greatest amount of distress in the pavements, as seen in Figure 21(b-c).

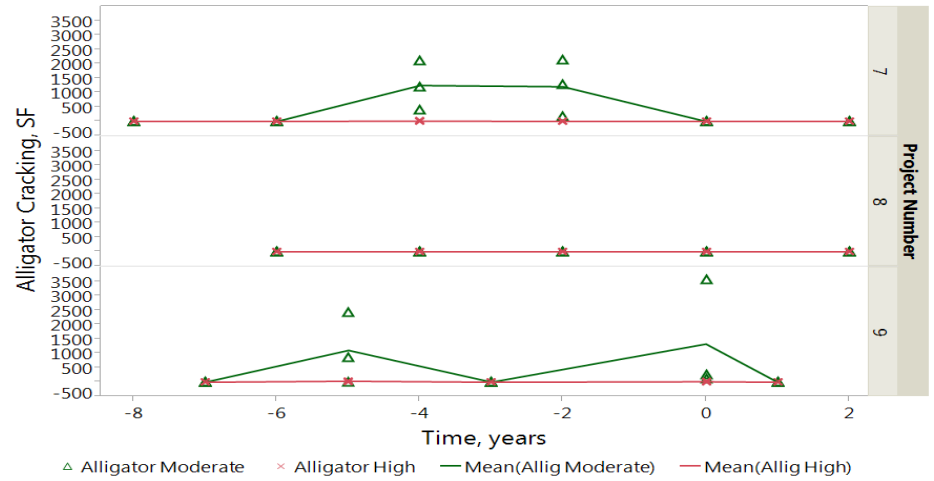

(a)

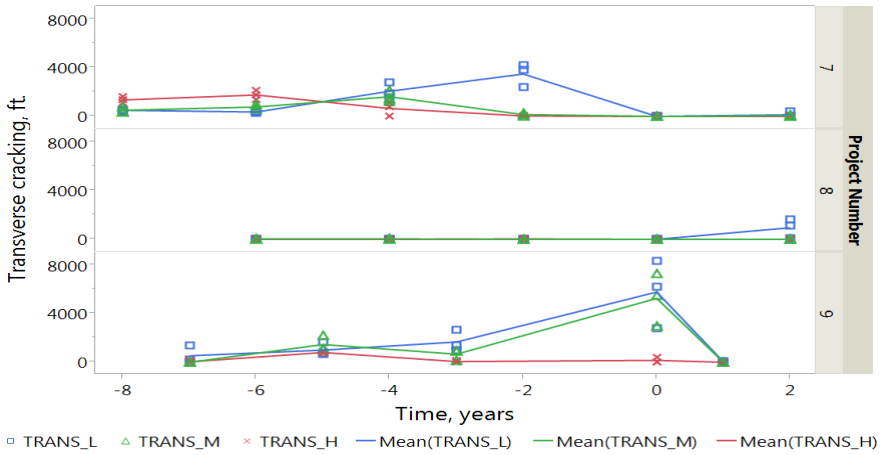

(b)

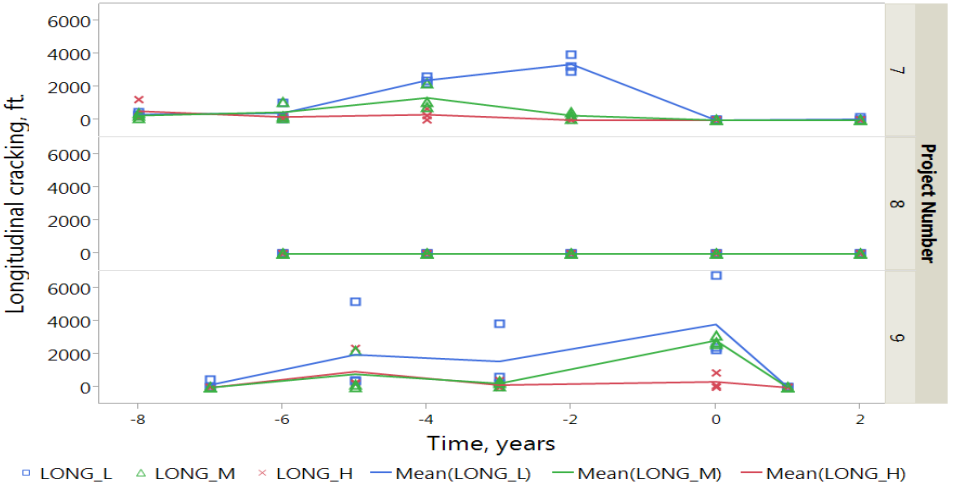

(c)

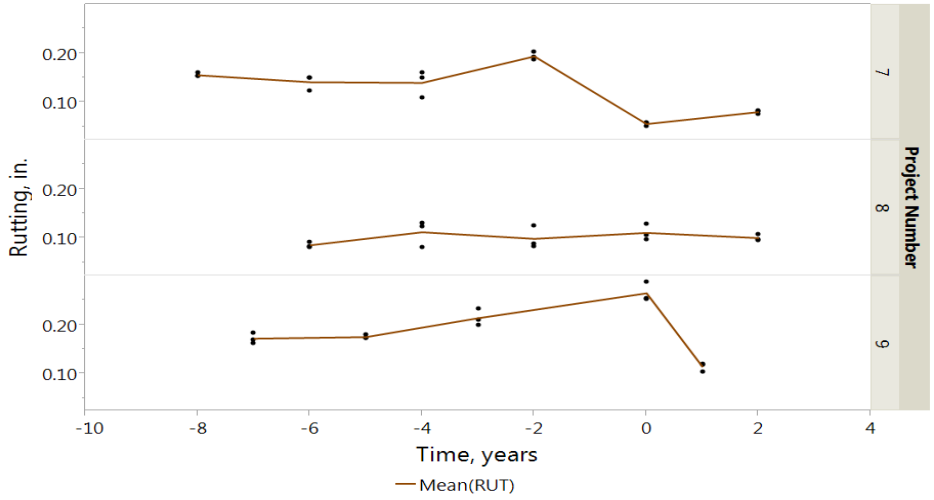

(d)

Figure 21: At 3M ESALs. (a) Alligator or Fatigue cracking, (b) transverse cracking, (c) longitudinal cracking, (d) rutting

10 Million ESALs

Projects 10, 11, and 12 pavement conditions are shown in Figure 22 at the top, middle and bottom, respectively. Project 12 showed no sign of fatigue, longitudinal and transverse cracking, as seen in Figure 22(a-c) top portion of the graph. Projects 10 and 11 show significant improvement in pavement performance after rehabilitation. In Figure 22(a), the fatigue cracking for both projects displayed similar trends; the average high severity cracking remained constant at zero while the average moderate cracking reached a peak two years prior to rehabilitation and subsequently decreased thereafter.

In Figure 23, the average IRI for all three projects were below 200 and remained relatively constant overtime. Figure 22(c) displayed large amounts of low severity longitudinal and transverse cracking in the pavement structure. The maximum low severity transverse cracking in project 11 was approximately double the maximum low severity longitudinal two years prior to rehabilitation; a similar trend in project 4, as shown in Figure#. Additionally, the transverse and longitudinal cracking for project 10 displayed similar trends in the level of severities. Figure 22(d), showed a slight increase in the average rutting in project 11 after rehabilitation, but none of the projects exceeded an average rutting depth of 0.17 inches.

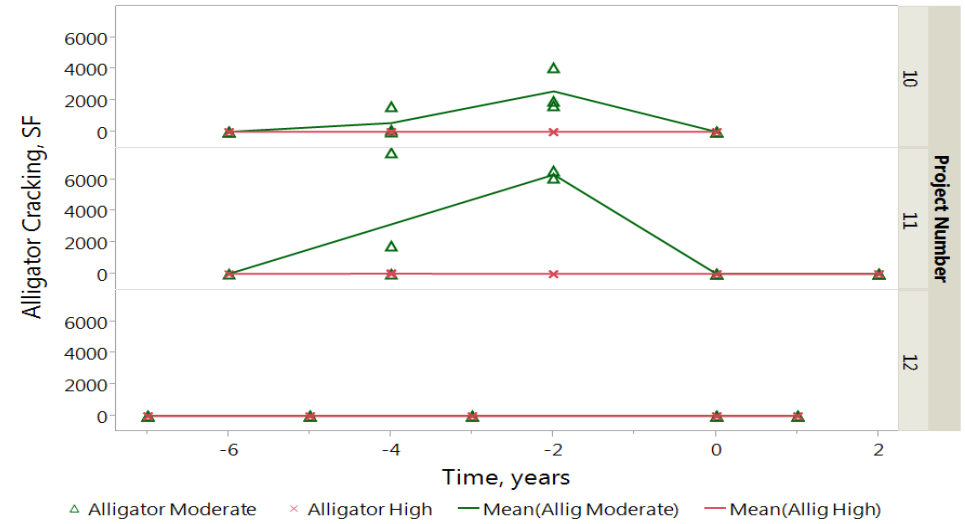

(a)

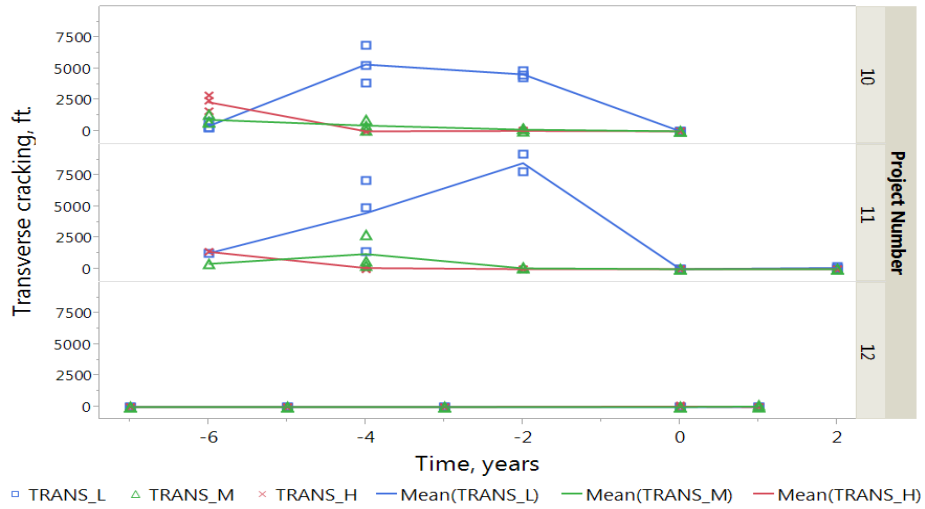

(b)

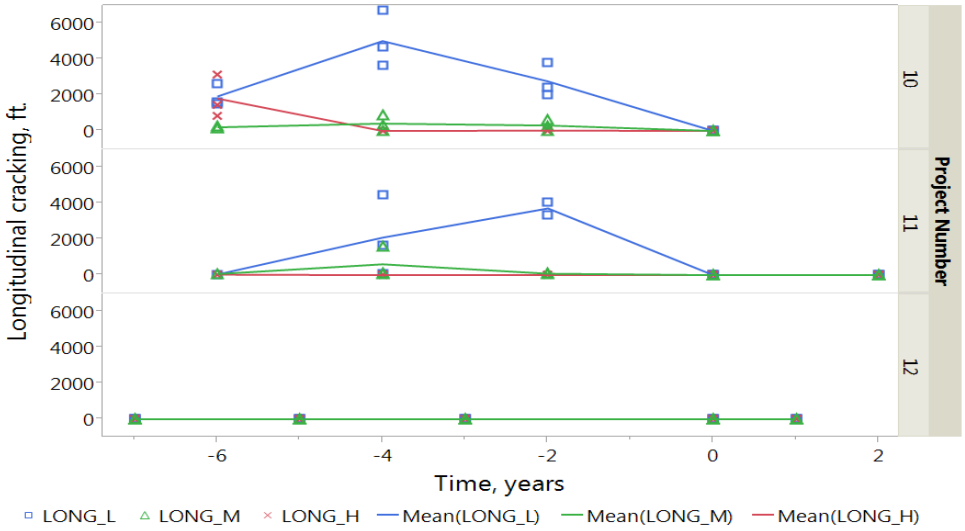

(c)

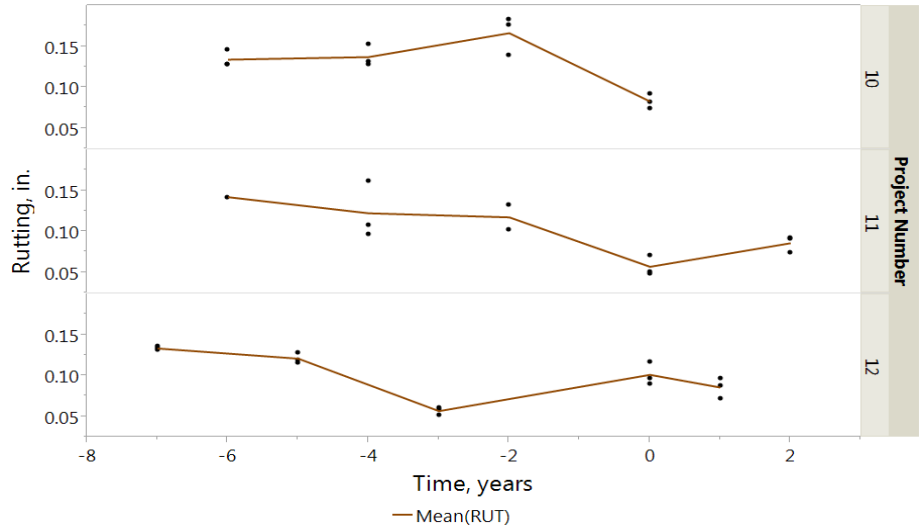

(d)

Figure 22: At 10M ESALs. (a) Alligator or Fatigue cracking, (b) transverse cracking, (c) longitudinal cracking, (d) rutting

For this research, IRI values were evaluated as shown in Figure 23. Pavement conditions post-rehabilitation for all projects showed significant improvement for all sections. PMIS data is collected on pavements in Iowa every two years and thus projects will continue to be evaluated under the State's PMIS program. The highest IRI was from the 1M ESAL mix in Clinton County. The post-construction IRI was highest for the 10 M ESAL Hamilton Co. project followed by Polk Co. Hwy 160 3M ESAL.

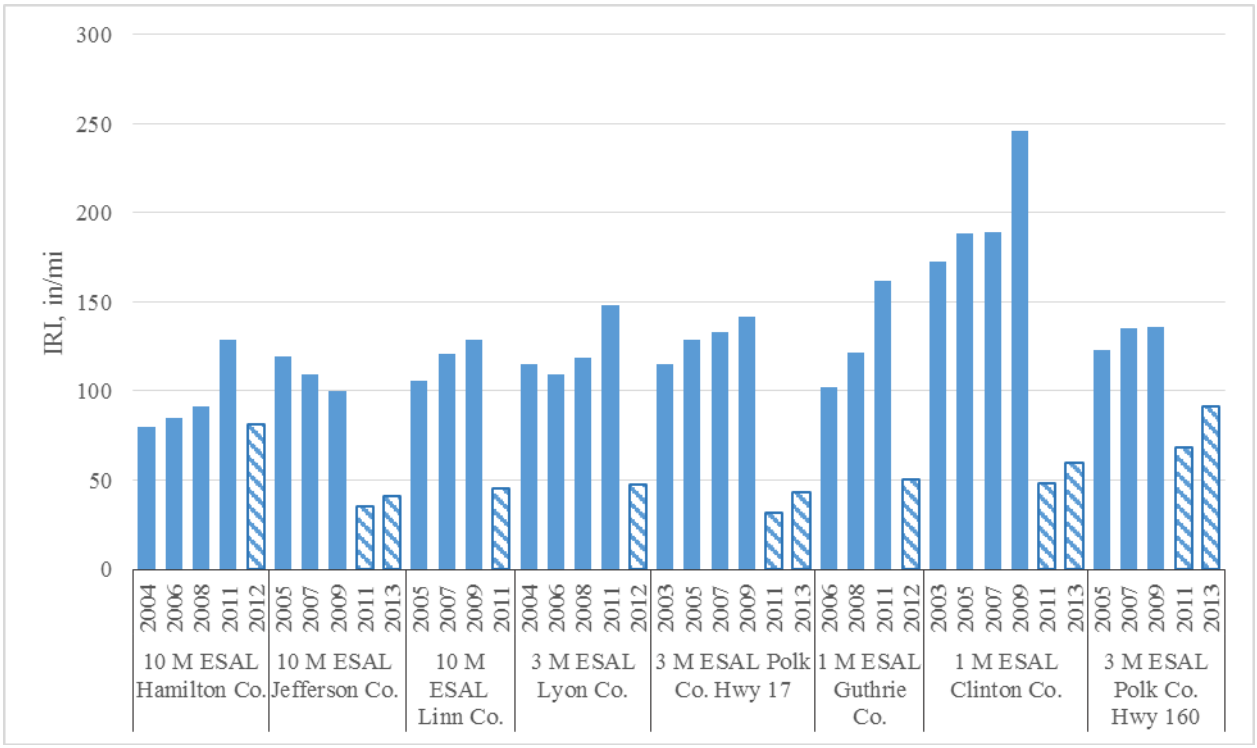

Figure 23: IRI indication at each ESAL levels

Theoretical maximum specific gravity QC/QA versus AASHTO T 209

The $G_{mm\ (QC/QA)}$ is the G_{mm} measured during QC/QA at construction and was used initially to estimate the field air voids at construction with the actual calculated G_{mb} from the field cores. It is expected that the values for $G_{mm\ (QC/QA)}$ would yield equivalent values of G_{mm} directly measured from the core. To verify, G_{mm} testing was carried out to validate if QC/QA G_{mm} values matched actual field core G_{mm} values. As shown in Figure 24 and Figure 25, based on the results, the percent air voids for $G_{mm\ (QC/QA)}$ yielded similar results to G_{mm} tested using AASHTO T209. The $G_{mm\ (QC/QA)}$ was also plotted against actual field G_{mm} with a linear fitted regression line. Figure 24 show that G_{mm} values 2.50 and below displayed better correlation between the observed values and predicted ($G_{mm\ (QC/QA)}$). Thus, for evaluating future air void information, the G_{mm} can accurately be used from QC/QA as opposed to conducting additional laboratory testing to validate the G_{mm} directly from field cores.

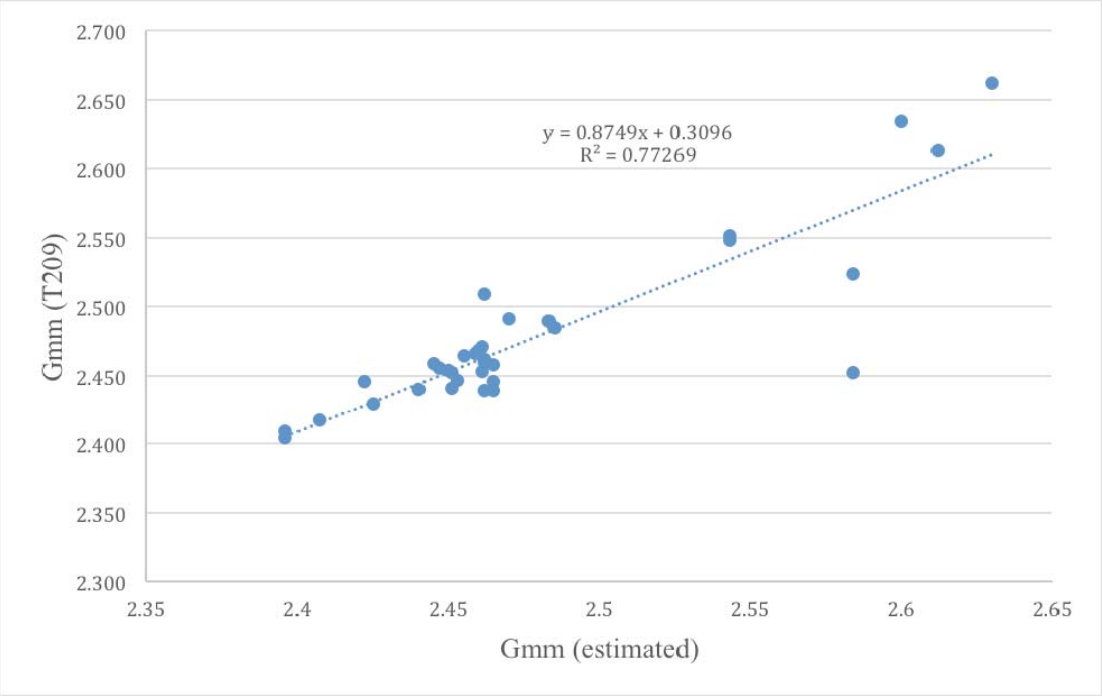

Figure 24: G_{mm} estimated or QC/QA versus actual G_{mm} or G_{mm} tested with AASHTO T209

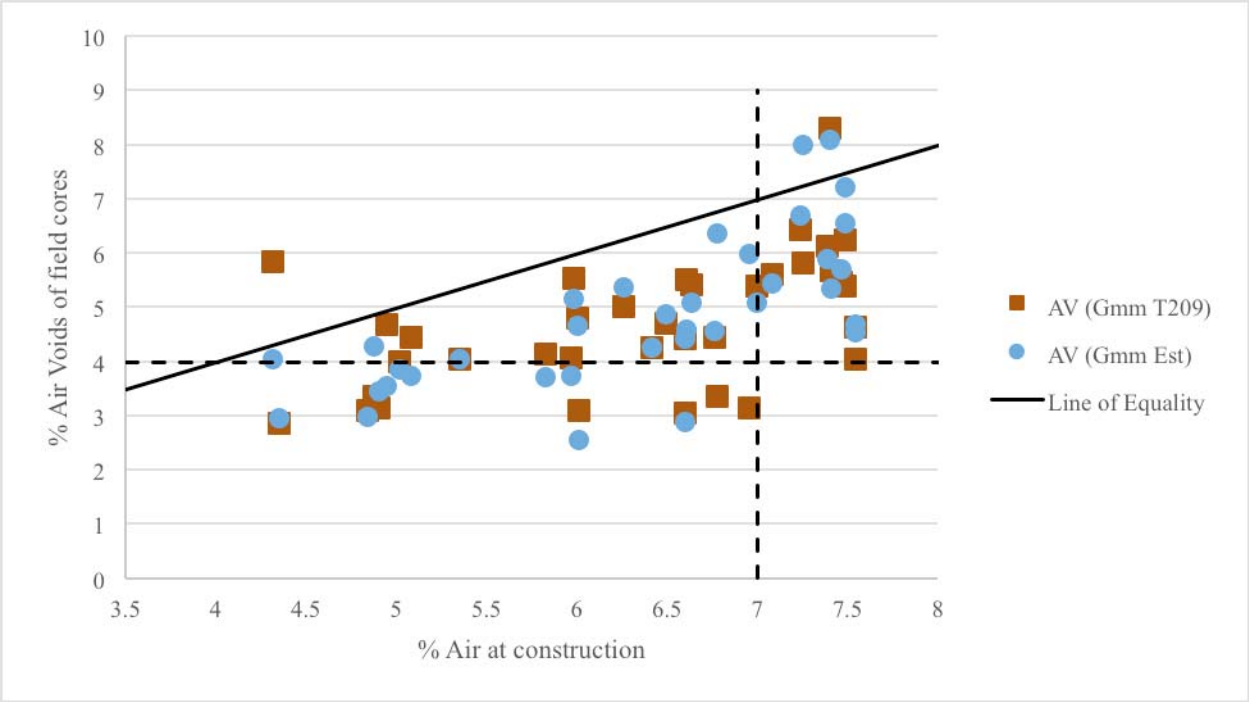

Figure 25: Calculated air voids with estimated G_{mm} from QC/QA data and air voids with G_{mm} measured from the field core tested in accordance to AASHTO T209

Change in Air Voids post-construction

The air voids at construction and field air voids were collected and analyzed for the research. The results show that air voids for 100-300K, 1M, 3M, and 10M ESALs four years post-construction displayed an average of less than 2.0 percent change in air voids. Figure 26(a-d) categorizes the change in air voids for each project by ESAL level.

The overall averages are shown in Figure 27(a) with the error bars representing the standard error (SE) bars of the change in air voids. Figure 27(b) shows the overall distribution of the change of air voids. From Figure 27(a), the change in air voids is similar for all mixes with the exception of 3M ESALs showing the highest average change. There were higher variations in

the change of air voids for ESAL levels 100-300K, 1M, and 3M compared to traffic levels at 10M ESALs. Traffic volumes at 3M ESALs tended to have higher change in air voids. One explanation may be the distribution of traffic on rural highways in the 3M ESAL category, IA 9 in Lyon county and Hwy 17 in Polk Co.

The average air voids four years post-construction for 100-300 ESALs was about 4.0% air voids, which indicate that the pavements under this specific ESAL level range reached ultimate pavement destiny. At construction, the air voids were compacted to an average of 6.0% at this ESAL level range. At 1M ESALs, although the average air voids at construction reached the initial target air voids of about 7.0%, the average air voids 4 years post-construction was about 5.0%. The results for 3M ESALs varied, specifically for projects paved in IA 160 in Polk Co (project 8). The overall average air voids four year post-construction and at construction was approximately 5.0% and 6.50% respectively. In project 8, the air voids at construction was roughly 5.0%, significantly lower than the desired initial target air voids compared to the other two projects. Pavement density for project 8 4 years post-construction reached to about 4.0% air voids, a 2 percent change in air voids. At 10M ESALs, the average air voids at construction for projects located in Hwy US 20 in Hamilton Co and Hwy US 34 in Jefferson Co (Projects 12 and 11 respectively) was about 7.30% air voids, which is above the initial target air voids; and the project located in Hwy US151 in Linn Co (Project 10) was overcompacted to about 5.0% air voids at construction. The air voids four years post-construction for projects 12 and 11 did not densify to 4% and final density was determined to be in the range of 6.20 – 6.80%, whereas in project 10, the air voids were approximately 3.0%. See Figure 28 for the average air voids per ESAL level 4 years post-construction and at construction.

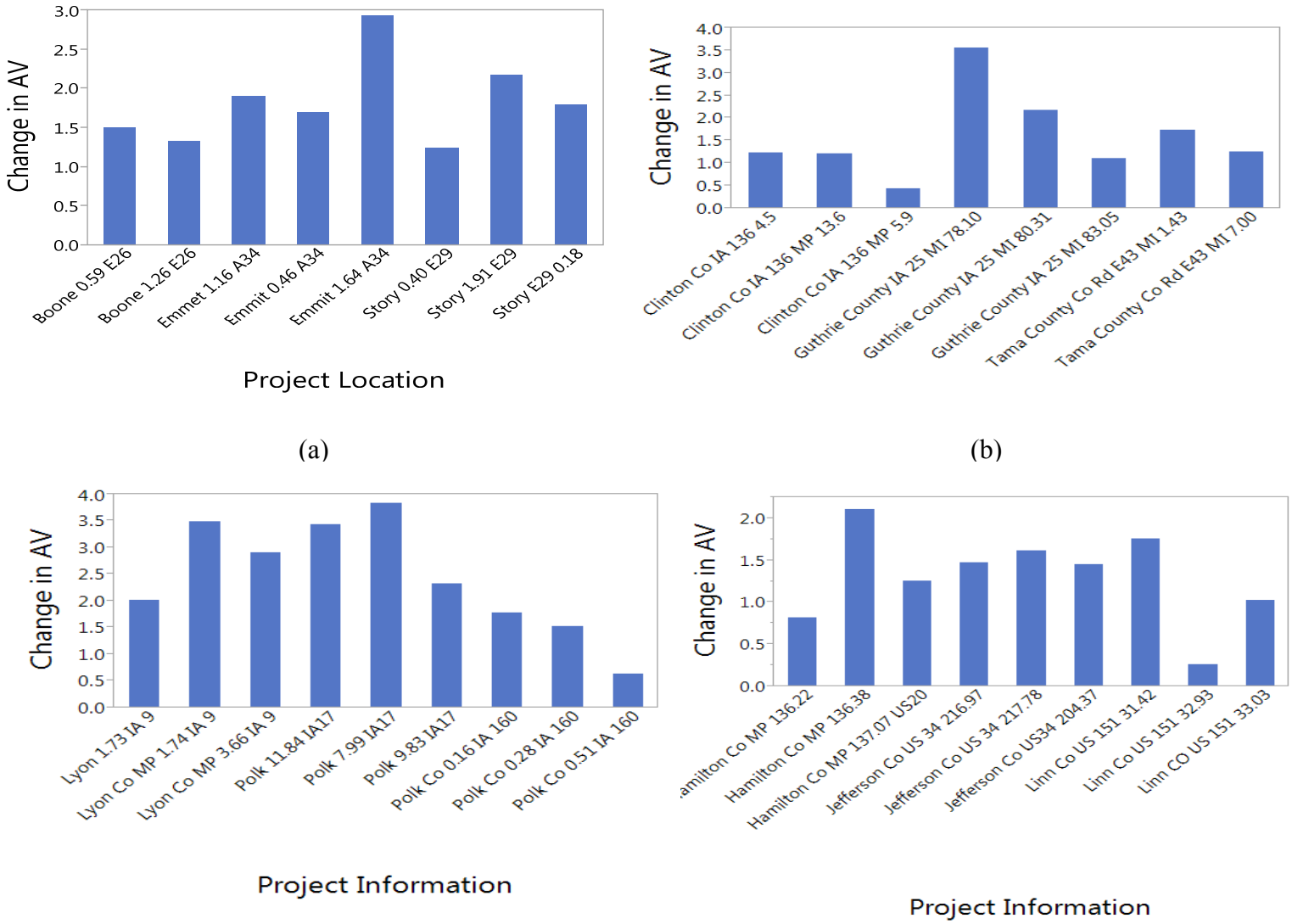

Figure 26: Change in percent air voids per ESAL level, (a) 100-300K, (b) 1M, (c) 3M, and (d) 10M

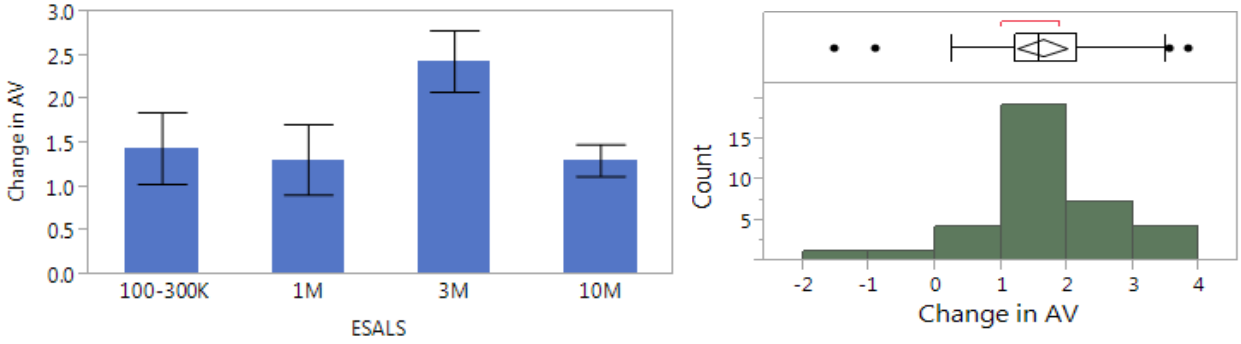

Figure 27: Change in percent air voids against ESALs (left). Distribution of the percent change in air voids with varying ESAL levels (right).

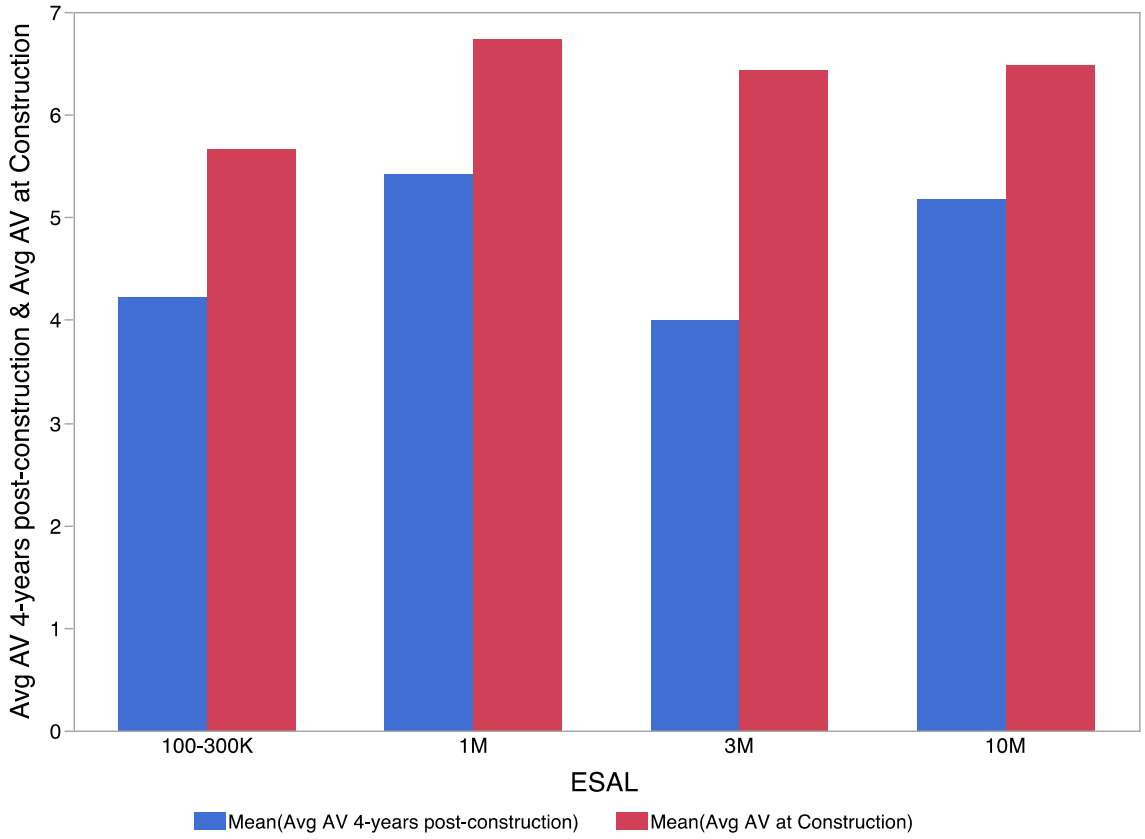

Figure 28: Average AV at construction and four years post-construction

Air Voids at construction and four years post-construction

The comparison between air voids at construction and air voids four years post-construction was evaluated. Figure 29 displays the overall percent air voids at construction plotted against percent air voids of the field cores four years post-construction. Based on the results, the ultimate pavement density has not been achieved for the majority of the projects. The percent air voids at construction plotted beyond 7% are unable to densify with traffic with the exception of one mixture. About 33% of the pavement sections for 1M and 3M ESALs as well as 56% for 10M ESALs of samples collected have not and will likely never reach the ultimate pavement density of 4%. Samples with traffic volume of 100-300K did not fall beyond the 7% air voids at construction. Only 11% of the samples collected reached the 4% target air voids, mainly projects at 100-300K ESALs. This can possibly be due to different aggregate specifications and requirements that generally allows for better compaction, such as higher criteria for fractures faces in a coarse aggregate angularity test, shape, texture, etc. As seen in Figure 29, the most problematic traffic levels were projects with 10M ESALs. Although projects with 100-300K ESALs were not compacted to 7% air voids at construction, 75% of the samples were within or significantly close to the target air void of 4% four years post-construction. The red circle solid line plotted beyond the 7% air voids at construction in Figure 29 represents the area of most concern.

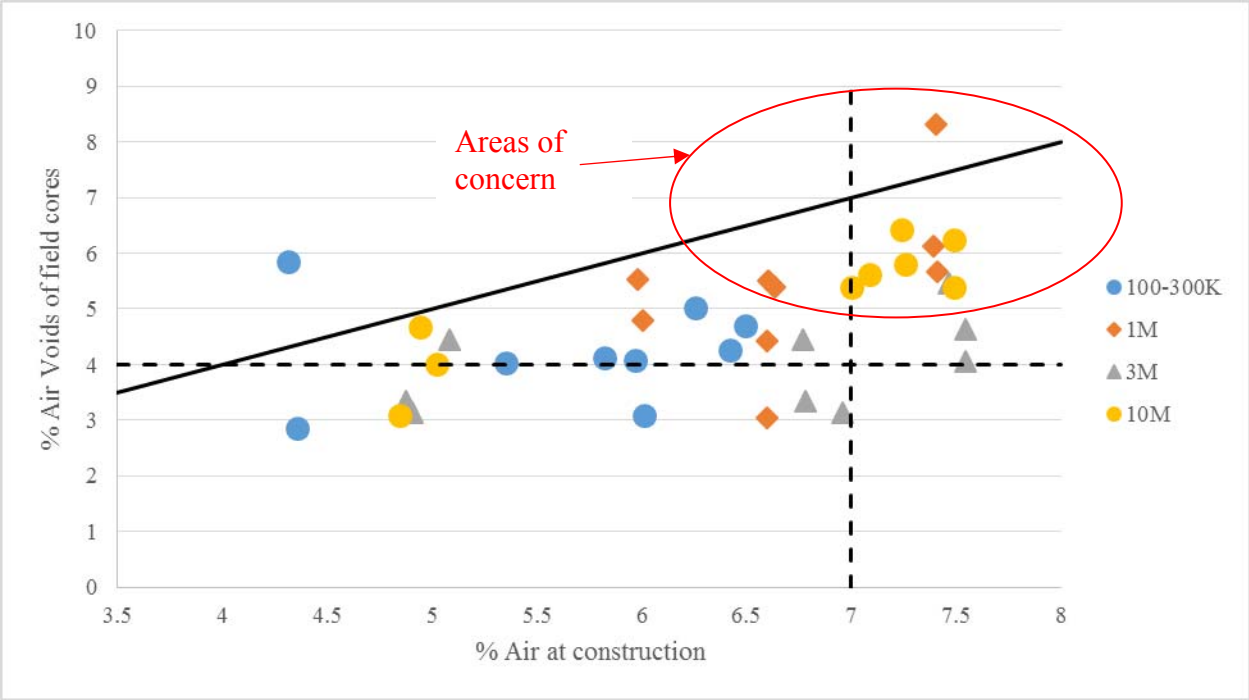

Figure 29: Percent air voids at construction versus air voids four years post-construction

Gyratory compaction slope and Post Construction Compaction Effort (PCCE)

The compaction slope for projects with available mix data is shown in Table 6. During the mix design, the N_{design} for 100-300K, 3M, and 10M were 68, 86, and 96, respectively. Mix designs are optimized for four percent target air voids or 96% G_{mm}. With the use of the slope for each mix and the percent G_{mm}, a theoretical compaction effort can be attained. A theoretical compaction effort is calculated using the $\%G_{mm}$ at construction and the gyratory slope; the parameter is designated $N_{@const.}$ In other words, $N_{@const.}$ represents the theoretical compactive effort in units of gyrations to represent the compactive effort achieved at the time of construction. Similarly, $N_{@4yrs}$ indicates the theoretical compactive effort in units of gyrations achieved four years post-construction. The difference in theoretical $N_{@4yrs}$ and $N_{@const.}$ represents

the applied post-construction compaction effort (PCCE). The concept is graphically displayed in Figure 30.

It is anticipated that as the mixes become more difficult to compact, the PCCE due to traffic loading will decrease because the mixes become less likely to compact under traffic. As shown in Figure 30, the lowest traffic volume, displayed the highest the PCCE that can be attributed to traffic and vice versa. At 100-300K ESALs, the PCCE was about 4.0% beyond the desired PCCE to achieve ultimate pavement density. The results validate that the pavement sections under this specific ESAL level range reached ultimate density 4 years post-construction. For 1M and 3M ESAL levels, the percent of PCCE was under the desired PCCE to reach target air voids and was only about 49% and 50% respectively below the required air voids at N_{design} at 96% G_{mm}. The most problematic ESAL level is 10M, which produced the highest percentage of 89% of PCCE required in order to reach ultimate pavement density. This indicates that at 10M ESALS, the projects were only able to densify at 11% 4 years post-construction, thus validating undercompaction during construction. Most projects at 10M ESALs were unable densify with traffic.

Due to the high variability within each ESAL level category, the projects were separately plotted for each ESAL level to better understand the effects of PCCE. Figure 31 shows the average $N_{@4yrs}$, $N_{@const.}$, and PCCE for each project selected. Based on this figure, there appears to be high variability within each project for a given ESAL level. The graph showed that the highest level of PCCE induced is at 100-300K ESALs at Emmit County. The results match the air voids analyses, where ultimate pavement density was achieved at ESAL levels 100-300K.

This indicates that higher PCCE was applied at these ESAL levels. While the higher ESAL levels varied in terms of PCCE, the results still indicate that target air voids four years post-construction was not reached with the use of the gyratory slope. Thus, the higher N_{design} levels will generally see a decrease in the post-construction compaction due to traffic.

Table 6: Compaction slope from mix data

Project No.	Project Location	ESALS	Gyratory Slope Semi log method N_{ini} to N_{des}
1	Boone E26	100-300K	6.651
2	Emmit A34	100-300K	6.363
3	Story E29	100-300K	6.382
4	Clinton Co IA 136	1M	5.859
5	Guthrie	1M	6.747
6	Tama	1M	6.393
7	Polk IA 17	3M	7.148
8	Polk Co IA 160	3M	6.414
9	Lyon Co IA 9	3M	5.680
12	Hamilton Co US 20	10M	7.899

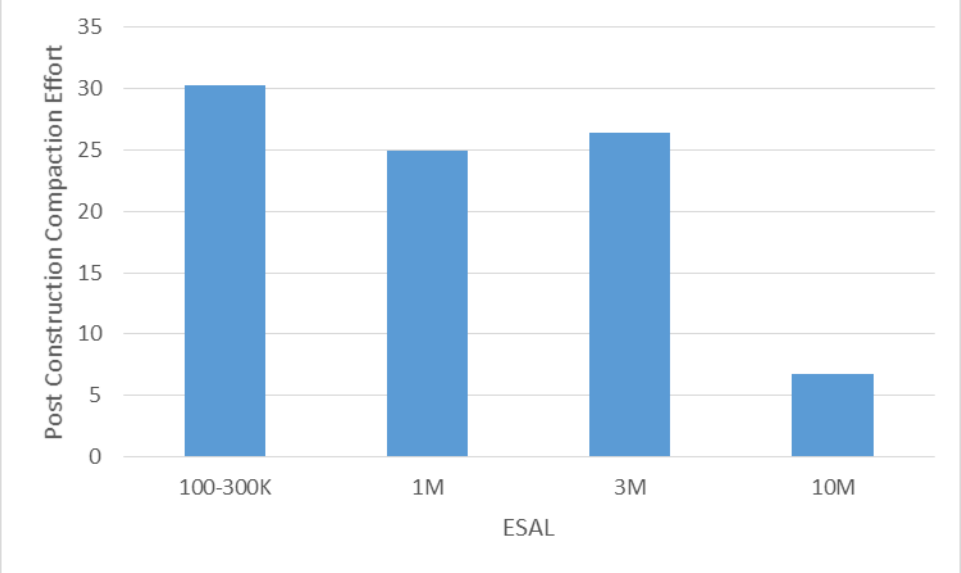

Figure 30: Post-construction compaction effort (PCCE) per ESAL level

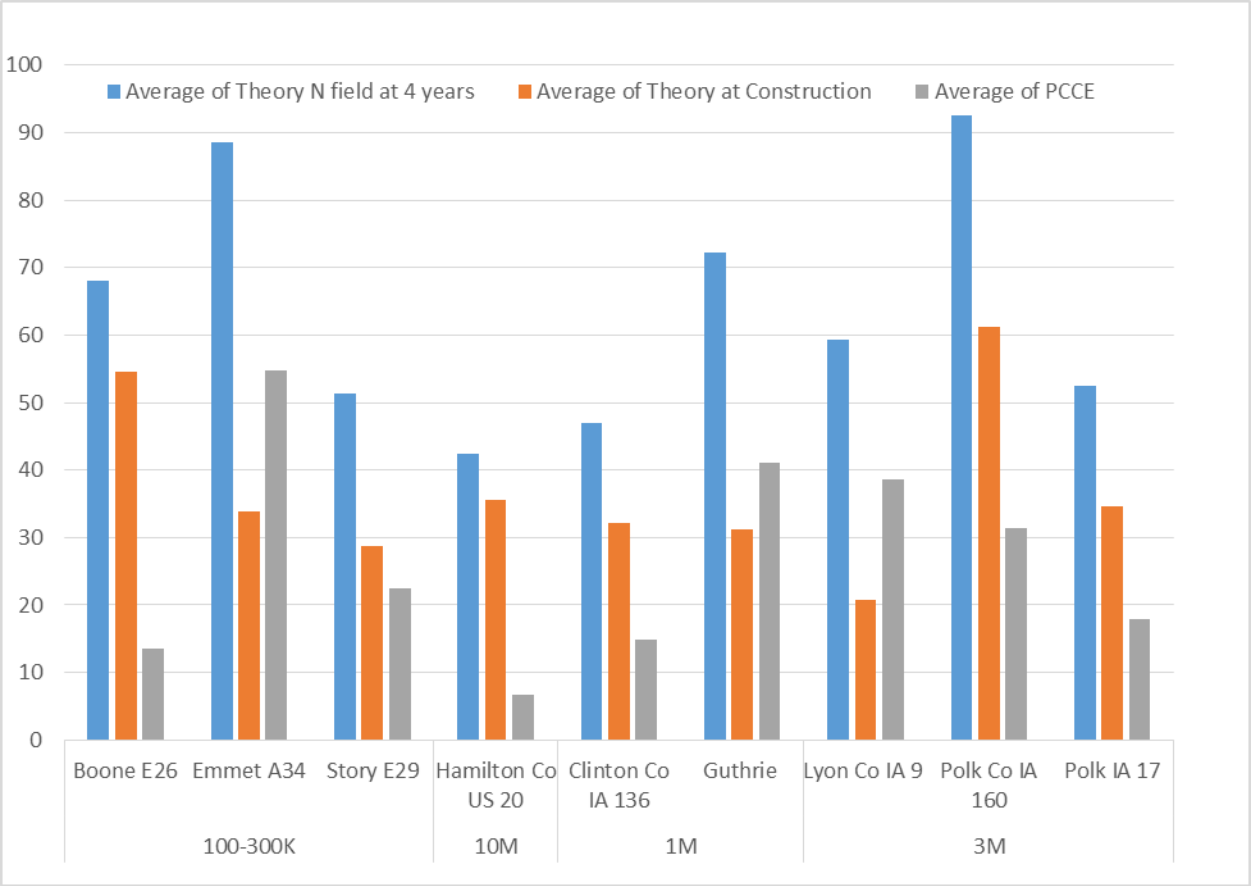

Figure 31: Average Theory $N_{@4yrs}$, $N_{@const.}$, and PCCE for each ESAL level

The previous analysis provides an estimate of how much densification from a pavement can be expected by traffic over a period of several years. The densification is expected and necessary for reducing the infiltration of water and improved pavement performance. On average, the change in air voids was approximately 1.75% from construction to four years post-construction. The highest average change observed was 2.5% for the 3M ESAL pavements. The analysis of air voids also showed that the higher air voids at construction had a decreased likelihood of ever reaching the 4% final air voids from the traffic compaction. The following histograms in Figure 32 show all $\%G_{mm}$ values at construction from 2011 to 2013 in the State of Iowa. The histograms indicate that there is a high probability that 25% of these pavements will

never reach 4% air void (or 96% G_{mm}). The histograms also show that the average percent G_{mm} in the field is 93.5%. The lower quartile is approximately 92.5% to 93.5%. If the average densification is applied and the distributions shifted, the average pavement will reach 95.25% densification. The shifted histogram shown in Figure 32 (solid line) indicate the predicted distribution of $\%G_{mm}$ four years post-construction for 2011, 2012 and 2013 based on the analyses conducted from the randomized field samples collected in 2011. This information provides an understanding of typical pavement densities in the field and how best to approach the N_{design} specification and continue to track the pavement densification process with time.

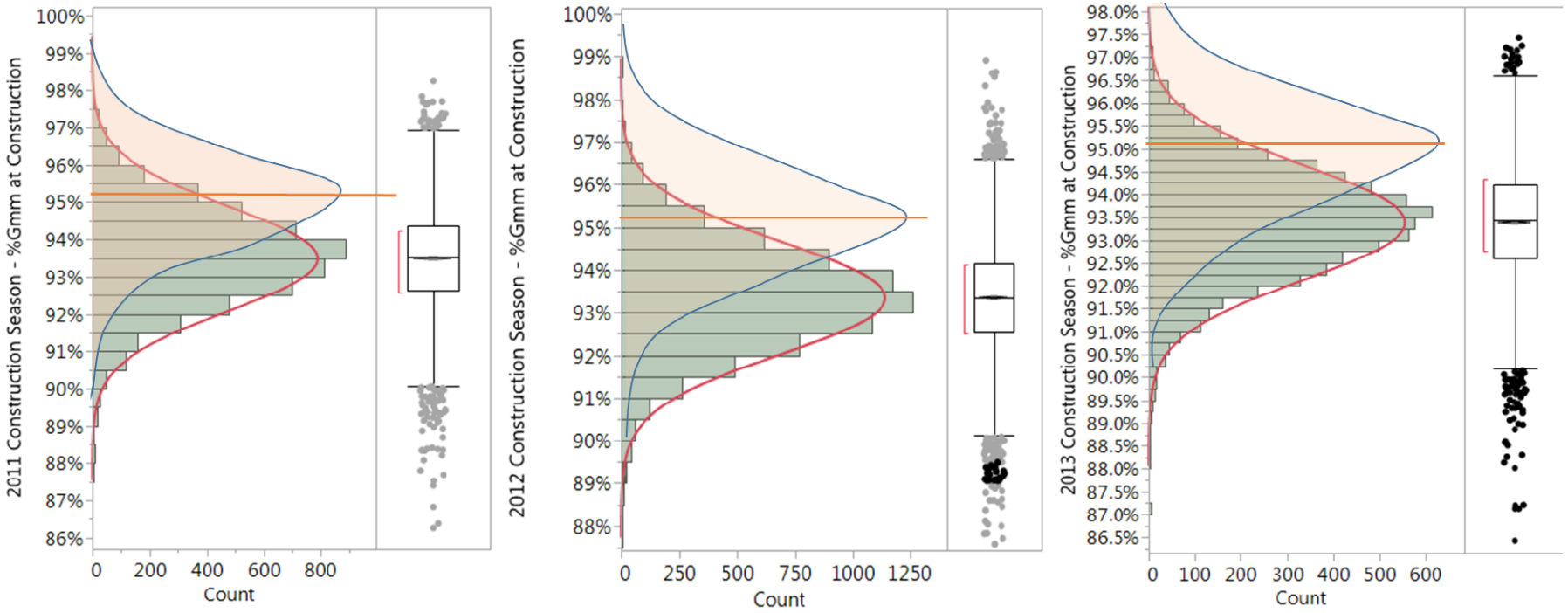

Figure 32: Distribution of % G_{mm} at construction with an expected shifted distribution for air voids at four years post-construction

CHAPTER 5: CONCLUSIONS AND RECOMMENDATIONS

Literature showed that the current N_{design} table in the Superpave Mix Design Method may possibly be too high in some instances. The challenge this creates is overcompaction during laboratory design leading to undercompaction in the field. Difficulty in compaction may result in decreased durability and increased water penetration.

This study found that within the selected projects, the overall pavement conditions showed significant improvements in pavement performance after rehabilitation in year 2011. No major pavement distresses were observed; the projects will be continuously monitored every two years. Additionally, the average decrease in air voids ranged between one and two percent and that majority of randomly selected locations did not reach 96% G_{mm} four years post-construction, specifically at the higher ESAL levels. A correlation between the density four years post-rehabilitation and performance of pavements in Iowa will be investigated in future research.

Based on the field and construction air voids analyses, for future study the G_{mm} from the QC/QA data can be utilized to determine the density of the pavement since the results show that field G_{mm} were close to the estimated G_{mm}. In addition, the study also showed that at the lowest ESAL level of 100-300K, the ultimate pavement density has been achieved at the design number of gyrations of 68. The outcome of the study showed that projects at the highest ESAL level of 10M displayed the most concern. Majority of the air voids at 10M ESALs were unable to densify with traffic due to undercompaction during construction. Projects at ESAL levels of 1M and 3M were also unable to reach ultimate pavement density with the current design number of

gyrations. Due to the undercomapction at construction, the target air voids of 4% is not always achieved within the four years for majority of the pavement locations studied.

Additionally, the post-construction compaction effort (PCCE), or estimated compaction due to traffic analysis validated the results obtained from the air voids analyses. The results showed that PCCE decreases with increasing traffic volumes. This indicates that higher ESAL levels become more difficult to compact and thus the mixes are less likely to compact under traffic. Preliminary results suggest a decrease in the number of design gyrations as the ones currently being used. Anomalies were present in the data analysis primarily in evaluating the gyratory and PCCE. There likely may be errors or miscalculations in the QC/QA data. Although there was high variability in determining the theory N four years post-construction, at construction and PCCE within each project the information is still valuable for the study.

Additional projects and mix design information will be valuable in further evaluating the findings of the study. Ongoing data collection from the PMIS data collection will also be useful in tracking how these pavements perform over time. Although more research is needed, the outcome of the research concluded that the pavements constructed with high gyration mix designs were less likely to achieve ultimate density in the field. In addition, based on the distribution of $\%G_{mm}$ at construction and the expected shifted distribution four years post-construction, the results estimated that there is a high probability that 25% of flexible pavements in Iowa will never reach ultimate pavement density; N_{design} being one of the major factors that contributes to this effect. As N_{design} standards are reconsidered for the State of Iowa, close attention to the design target air voids and VMA will be addressed. Future research will be

conducted to validate and recommend the optimum design number of gyrations in Iowa. Phase II will consist of laboratory work and the determination of the N_{design} used to obtain ultimate pavement density.

REFERENCES

1. *AFG2AS/AFG2CS Superpave Gyratory Compactor Operation Manual Pine Instrumental Company*. Pine Instrumental Company.
2. *Why Concrete Races Differently than Asphalt*, S.d.s.i. red, Editor. 2012.
3. Harmelink, D. and T. Aschenbrener, *In-Place Voids Monitoring of Hot Mix Asphalt Pavements*. 2002, Colorado Department of Transportation Research Branch.
4. Prowell, B.D. and R.E. Brown, *Superpave Mix Design: Verifying Gyration Levels in the Ndesign Table*. 2007, Transportation Research Board.
5. Brown, E.R., et al., *Hot Mix Asphalt Materials, Mixture Design and Construction*, ed. T. Edition. 2009, Lanham, Maryland: NAPA Research and Education Foundation. 311.
6. Christensen, D.W. and R. Bonaquist, *Rut Resistance and Volumetric Composition of Asphalt Concrete Mixtures*, in *Association of Asphalt Paving Technologists*. 2005.
7. Hmoud, H.R., *Evaluation of VMA and Film Thickness Requirements in Hot-Mix Asphalt.* Modern Applied Sciences, 2011. **5**(4): p. 166.
8. Institue, A., *Superpave Mix Design No. 2*. Vol. 2. 2001.
9. *History of Asphalt*. National Asphalt Pavement Association 2015 [cited 2015; Available from: https://www.asphaltpavement.org/index.php?option=com_content&view=article&id=21&Itemid=41.
10. Peterson, R.L., et al., *Superpave Laboratory Compaction Versus Field Compaction.* Transportation Research Board: Journal of the Transporation Research Board, 2003. **1832**(1): p. 201-208.
11. Huang, Y.H., *Pavement Analysis and Design*, ed. n. Edition. 2003.
12. Anderson, M.R., et al., *Relationship of Superpave Gyratory Compaction Properties to HMA Rutting Behavior*, in *NCHRP Report 478*. 2002, Transportation Research Board: Washington, D.C.
13. Maupin, G.W., *Additional Asphalt to Increase the Durability of Virginia's Superpave Surface Mixes*. 2003, Virginia Transportation Research Council Virginia Department of TransportationUniversity of Virginia Federal Highway Administration: Charlottesville, Virginia.
14. Hornbeck, N.C., *Effect of Compaction Effort on Superpave Surface Course Materials*, in *Civil and Environmental Engineering*. 2008, West Virginia University: Morgantown, West Virginia.
15. Anderson, M.R., D.W. Christensen, and R. Bonaquist, *Estimating the Rutting potential of Asphalt mixtures using SGC properties and IDT*. 2003.
16. Aguiar-Moya, J.P., J.A. Prozzi, and M. Tahmoressi, *Optimum Number of Superpave Gyrations Based on Project Requirements.* Transportation Research Record: Journal of the Transportation Research Board, 2001: p. 84-92.

17. Watson, D.E., et al., *Verification of Superpave Number of Design Gyration Compaction Levels for Georgia.* Transportation Research Record: Journal of the Transportation Research Board, 2008. **2057**(1): p. 75-82.
18. *Construction and Material Specification*. 2013, Department of Transportation Columbus, Ohio.
19. Interactive, P., *Rutting*, F.S.m. rutting, Editor. 2008.
20. Management, P., *Fatigue Cracking* 2009.
21. *Pavement Distress*, B. cracking, Editor.
22. Miller, J.S. and W.Y. Bellinger, *Distress Identification Manual for the Long-Term Pavement Performance Program* 2003.
23. D2726M, A.S.D., *Standard Test Method for Bulk Specific Gravity and Density of Non-Absorptive Compacted Bituminous Mixtures*.
24. T209, A., *Theoretical Maximum Specific Gravity and Density of Hot Mix Asphalt*. 2015.
25. Transportation, I.D.o., *Iowa Interstate Corridor Plan*. 2013.

APPENDIX A: QC/QA FIELD VOIDS DATA

Table 7: QC/QA field voids data for selected projects

County	Project No.	IDOT Project No.	Core#/Station	Intended Thickness, in.	Actual Thickness, in.	G_{mm} (est.)	AV @ const, %	ESAL	N_{design}
Boone	1	FM-C008(55)--55-08	2/288+10	1.5	1.8	2.462	4.509	100-300K	68
			3/297+18	1.5	2	2.462	4.468		
			4/323+23	1.5	1.7	2.466	5.312		
Emmet	2	STP-S-CO32--5E-32	4/61+31	N/A	2	2.396	5.968		
			7/86+61	N/A	1.825	2.396	6.010		
			3/24+56	N/A	1.75	2.407	5.941		
Story	3	STP-S-C085(107)--5E-85	8/21+69	1.5	1.6	2.461	6.258		
			5/101+19	1.5	1.6	2.462	6.418		
			8/9+80	1.5	1.6	2.465	6.491		
Clinton	4	STP-136-1(63)--2C-23	3/254+98	2	2	2.461	6.136	1M	76
			8/664+05	2	2	2.45	6.122		
			8/182+93	2	1.875	2.46	6.179		
Guthrie	5	STP-025-4(40)--2C-39	7/223+98	1.5	1.7	2.425	6.598		
			5/340+97	1.5	1.875	2.44	6.598		
			4/485+60	1.5	1.84	2.422	6.606		
Tama	6	STP-S-CO86(077)--5E-86	7/286+12	1.5	1.52	2.458	7.404		
			5/369+35	1.5	1.75	2.449	7.391		
			3/75+54	1.5	1.48	2.457	7.407		

Table 8: Cont. of QC/QA field voids data for selected projects

County	Project No.	IDOT Project No.	Core#/Station	Intended Thickness, in.	Actual Thickness, in.	G_{mm} (est.)	AV @ const, %	ESAL	N_{design}
Polk	7	STP-017-1(16)--2C-77	3/237+83	2	1.5	2.468	6.767	3M	86
			6/8+38	2	2.1	2.487	6.956		
			2/131+62	2	1.9	2.478	6.780		
Polk	8	STP-160-1(10)--2C-77	1/344.68	2	1.7	2.468	4.903		
			2/301.66	2	2.1	2.463	4.872		
			2/356.83	2	2.2	2.441	5.080		
Lyon	9	STP-009-1(39)--2C-60	7/92+27	1.5	1.63	2.452	7.463		
			4/193+93	1.5	1.38	2.453	7.542		
			8/92+65	1.5	1.63	2.453	7.542		
Linn	10	NHSX-151-3(119)--3H-57	3/171+75	2	1.75	2.63	4.981	10M	96
			4/176+67	2	1.75	2.63	5.057		
			5/92+23	2	2	2.605	4.952		
Jefferson	11	NHSX-034-8(143)--3H-51	4/920+52	1.5	1.625	2.541	7.084		
			8/977+65	1.5	1.5	2.558	6.998		
			1/105+65	1.5	1.875	2.577	7.256		
Hamilton	12	MP-020-1(705)136--76-40	2/12+38	2	1.7	2.47	7.490		
			6/48+60	2	1.9	2.471	7.487		
			1/3+80	2	1.9	2.46	7.236		

APPENDIX B: QC/QA LABORATORY VOIDS

Table 9: QC/QA laboratory voids data for selected projects

			CON		IDOT				
County	Project No.	IDOT Project No.	G_{mm}	AV	G_{mb}	G_{mm}	AV	ESAL	N_{design}
Boone	1	FM-C008(55)--55-08	2.458	3.295	2.383	2.463	3.248	100-300K	68
			2.461	2.966					
			2.466	3.487					
			2.466	3.933	2.365	2.463	3.979		
			2.467	3.486					
			2.466	3.690					
Emmet	2	STP-S-CO32--5E-32	2.404	3.494	2.327	2.406	3.283		
			2.41	3.402					
			2.396	3.005	2.33	2.405	3.119		
			2.396	2.379					
			2.396	2.462					
			2.396	3.005	2.33	2.405	3.119		
			2.396	2.379					
			2.396	2.462					
Story	3	STP-S-C085(107)--5E-85	2.46	3.577	2.379	2.467	3.567		
			2.461	3.210					
			2.461	3.291					
			2.465	3.773					
			2.462	3.940	2.366	2.45	3.429		
			2.462	3.940					
			2.461	3.413					

Table 10: Cont. of QC/QA laboratory voids data for selected projects

			CON		IDOT				
County	Project No.	IDOT Project No.	G_{mm}	AV	G_{mb}	G_{mm}	AV	ESAL	N_{design}
Clinton	4	STP-136-1(63)--2C-23	2.472	4.814				1M	76
			2.457	4.070					
			2.45	3.429	2.375	2.452	3.140		
			2.457	3.541	2.383	2.453	2.854		
			2.465	4.016					
			2.464	3.977					
			2.456	3.705					
			2.447	3.515					
			2.454	3.708	2.375	2.452	3.140		
			2.45	3.592					
Guthrie	5	STP-025-4(40)--2C-39	2.43	3.416					
			2.424	3.218					
			2.422	3.303					
			2.435	3.737	2.347	2.433	3.535		
			2.441	3.523					
			2.442	3.890					
			2.442	3.931					
			2.416	2.649	2.353	2.425	2.969		
			2.423	2.889					
			2.428	3.542					
Tama	6	STP-S-CO86(077)--5E-86	2.459	4.189					
			2.457	4.151					
			2.465	4.706					
			2.454	3.953	2.345	2.451	4.325		
			2.452	4.119					
			2.451	3.835					
			2.462	4.184	2.34	2.454	4.645		
			2.449	4.328					
			2.448	4.616	2.323	2.45	5.184		
			2.446	4.579					
			2.445	4.540					

Table 11: Cont. of QC/QA laboratory voids for selected projects 7-12

			CON		IDOT				
County	Project No.	IDOT Project No.	G_{mm}	AV	G_{mb}	G_{mm}	AV	ESAL	N_{design}
Polk	7	STP-017-1(16)--2C-77	2.468	3.687	2.393	2.458	2.644	3M	86
			2.472	3.681	2.406	2.455	1.996		
			2.487	4.584					
			2.488	4.582	2.397	2.476	3.191		
			2.482	3.948					
			2.483	3.947					
			2.478	3.672					
			2.487	4.423	2.388	2.48	3.710		
Polk	8	STP-160-1(10)--2C-77	2.474	3.032	2.389	2.475	3.475		
			2.481	3.426					
			2.483	3.907					
			2.478	4.036	2.368	2.475	4.323		
			2.486	3.781					
			2.488	4.100					
Lyon	9	STP-009-1(39)--2C-60	2.446	3.802					
			2.45	3.837					
			2.453	3.954					
			2.453	4.117	2.342	2.452	4.486		
			2.45	4.204					
			2.454	4.482					
			2.456	4.886	2.321	2.448	5.188		
			2.452	4.812				10M	96
Linn	10	NHSX-151-3(119)--3H-57	2.603	3.419					
			2.602	3.420	2.522	2.608	3.298		
			2.633	5.735					
			2.609	4.446					
			2.629	3.576					
			2.63	3.460					
Jefferson	11	NHSX-034-8(143)--3H-51	2.577	3.454					
			2.59	4.595	2.488	2.582	3.641		
			2.529	3.440	2.454	2.53	3.004		
			2.541	3.817					
			2.558	4.730					
Hamilton	12	MP-020-1(705)136--76-40	2.469	4.617	2.36	2.473	4.569		
			2.46	4.593					
			2.47	4.332	2.37	2.47	4.049		
			2.46	3.455					

APPENDIX C: RAW DATA FOR AIR VOID ANALYSES

Table 12: Data for air void analyses

Project Location	Average of Ndes	Avg AV 4yrs post-const.	Average of AV at const.	Average of AADT	% G_{mm} at 0 years	% G_{mm} at 4 years	Change AV
Boone E26	68	2.859	4.353	690	95.647	97.053	1.495
Boone E26	68	5.841	4.312	690	95.688	95.959	-1.528
Boone E26	68	4.029	5.351	690	94.649	95.971	1.322
Emmet A34	68	4.068	5.968	320	94.032	96.259	1.901
Emmet A34	68	4.128	5.824	320	94.176	96.295	1.695
Emmet A34	68	3.085	6.010	730	93.990	97.456	2.925
Story E29	68	5.016	6.258	560	93.742	94.643	1.242
Story E29	68	4.255	6.418	560	93.582	95.755	2.163
Story E29	68	4.701	6.491	560	93.509	95.140	1.790
Clinton Co IA	76	5.402	6.634	1230	93.366	94.912	1.233
Clinton Co IA	76	4.797	6.007	2110	93.993	95.345	1.210
Clinton Co IA	76	5.535	5.983	1230	94.017	94.852	0.448
Guthrie County IA 25	76	3.040	6.598	1100	93.402	97.125	3.557
Guthrie County IA 25	76	4.420	6.598	1100	93.402	95.581	2.179
Guthrie County IA 25	76	5.500	6.606	1100	93.394	95.415	1.106
Tama County Co Rd E43	76	5.674	7.407	740	92.593	94.660	1.733
Tama County Co Rd E43	76	8.309	7.404	740	92.596	91.923	-0.905
Tama County Co Rd E43	76	6.126	7.391	740	92.609	94.125	1.265
Lyon IA 9	86	5.453	7.463	3290	92.537	94.296	2.010
Lyon IA 9	86	4.046	7.542	3290	92.458	95.476	3.496
Lyon IA 9	86	4.636	7.542	3290	92.458	95.320	2.905

Table 13: Cont. of data for air void analyses

Project Location	Average of Ndes	Avg AV 4yrs post-cont.	Average of AV at const.	Average of AADT	% G_{mm} at 0 years	% G_{mm} at 4 years	Change AV
Polk IA17	86	3.350	6.780	980	93.220	93.645	3.430
Polk IA17	86	3.127	6.956	980	93.044	94.025	3.829
Polk IA17	86	4.440	6.767	980	93.233	95.434	2.327
Polk Co IA 160	86	3.127	4.903	21600	95.097	96.559	1.775
Polk Co IA 160	86	3.350	4.872	21600	95.128	95.717	1.522
Polk Co IA 160	86	4.440	5.080	21600	94.920	96.268	0.640
Hamilton Co US20	96	6.418	7.236	8200	92.764	93.301	0.818
Hamilton Co US20	96	5.385	7.490	8200	92.510	93.451	2.105
Hamilton Co US20	96	6.234	7.487	8200	92.513	92.793	1.253
Jefferson Co US 34	96	5.610	7.084	5200	92.916	94.575	1.473
Jefferson Co US 34	96	5.381	6.998	5200	93.002	94.932	1.617
Jefferson Co US 34	96	5.805	7.256	6600	92.744	92.000	1.451
Linn Co US 151	96	3.083	4.842	7300	95.158	97.018	1.760
Linn Co US 151	96	4.684	4.945	7300	95.055	96.464	0.261